1974

Direct and inverse heat conduction in rock materials using the finite element method

Vernon Dale Allen

DIRECT AND INVERSE HEAT CONDUCTION IN ROCK MATERIALS USING THE FINITE ELEMENT METHOD

by

VERNON DALE ALLEN, 1941-

A DISSERTATION

Presented to the Faculty of the Graduate School of the

UNIVERSITY OF MISSOURI-ROLLA

In Partial Fulfillment of the Requirements for the Degree

DOCTOR OF PHILOSOPHY

in

MECHANICAL ENGINEERING

1974

Jerry T. Lehnhoff
Advisor

R. T. Johnson

S. Bagavi

George B. Clark

Harold VanKeith

ABSTRACT

A finite element method is presented for solution of direct and inverse heat conduction problems in rock materials. Finite element programs for direct and inverse heat conduction problems were developed and demonstrated. Flow charts are given for the finite element programs.

The direct finite element heat conduction program changes material properties with temperature to approximate the temperature dependent properties of rock materials. An example problem was solved by the finite element method and also using Kirchoff's transformation. The finite element solution compared quite well with the Kirchoff transformation solution.

The inverse method utilizes the direct finite element heat conduction program to iterate for the inverse solution. Data to test the inverse finite element program was generated with the direct finite element program of this research. The inverse program solved these generated problems very accurately.

Internal temperature and fracture time measurements are presented on a series of hollow Dresser Basalt cylinders heated by a Kanthal wire heater. The internal temperature measurements were used in conjunction with the inverse method to obtain surface temperatures. The surface temperatures were used for thermal stress calculations to obtain time to fracture for an infinite cylinder.

ACKNOWLEDGEMENTS

The author wishes to express his appreciation to Dr. Terry F. Lehnhoff for suggestions in preparation of this dissertation. Gratitude is also extended to the Ph.D advisory committee, Professor S.J. Pagano and Drs. G.B. Clark, H.D. Keith and R.T. Johnson. Special thanks are extended to Mr. Jaw K. Wang for drawing the figures of this dissertation.

The author is grateful to the Rock Mechanics and Explosives Research Center and the Department of Mechanical Engineering for financial support provided in the form of Graduate Research and Teaching Assistantships.

Finally, sincere appreciation is extended to my wife, Cheryl, for her patience during this research and for cheerfully typing this dissertation.

TABLE OF CONTENTS

Page

ABSTRACT ii

ACKNOWLEDGEMENT iii

LIST OF ILLUSTRATIONS vii

LIST OF TABLES ix

NOMENCLATURE AND LIST OF SYMBOLS x

I. INTRODUCTION 1

A. The Need for Thermal Analysis of Rock Materials 1

B. The Direct Method of Heat Transfer for Rock Materials 3

C. The Inverse Method of Heat Transfer 5

D. Discussion of Fracture Considerations . 18

E. Material Properties 20

F. Influence of Thermocouples on Measured Temperature 23

G. Objective and Scope 23

II. THE DIRECT METHOD 25

A. Linear Finite Element Equations 25

B. Linear Approximation for the Non-linear Case 26

C. Comparison of a Linearized Finite Element Method Solution to Kirchoff Transformations 28

D. Steady State Analysis 30

E. Alternate Steady State Procedure 33

F. Finite Element Program 34

Table of Contents (continued) Page

III. THE INVERSE METHOD OF HEAT CONDUCTION 37

A. Mathematical Formulation of the Inverse Problem for Solution by Iteration of a Direct Solution 37

B. Evaluation of Improvement dg 43

C. Iteration Solution 45

D. Particular Examples of the Inverse Method 48

E. Inverse Finite Element Program 54

IV. FUTURE TIME CONSIDERATIONS BASED ON WAVE SPEEDS 57

A. Calculation of Delay Time 59

B. Future Times for Use with Numerical Solutions 63

V. EXPERIMENTAL DATA 66

A. Discussion of the Experimental Example 66

B. Experimental Temperature Data 74

C. Experimental Fracture Data 76

D. Supplemental Tests 78

VI. APPLICATION OF THE INVERSE METHOD 80

A. Boundary Condition g 80

B. Boundary Condition Improvement 82

C. Finite Element Models 82

D. Future Times 89

E. Results of the Inverse for Experimental Example 89

F. Fracture Prediction Based on the Inverse Solution 92

Table of Contents (continued) Page

VII. CONCLUSIONS AND RECOMMENDATIONS 95

A. Conclusions 95

B. Recommendations 95

BIBLIOGRAPHY 97

VITA 103

APPENDICES 104

A. Thermal Analysis Program, 2DNLT - Input Instructions 104

B. Surface Improvements 110

C. Inverse Thermal Analysis Program, INVRS - Input Instructions 113

D. Experimental Equipment and Wiring Diagrams 120

LIST OF ILLUSTRATIONS

Figures Page

1. Comparison of Linearized Finite Element Program (2DNLT) Solution with Kirchoff Transformation Solution 31

2. Convergence of Linearized Finite Element Program (2DNLT) Solution and Convergence of Kirchoff Transformation Solution 32

3. Flow Chart (2DNLT) 35

4. Temperature Distribution across the Cylinder after .05 Seconds 50

5. Temperature History at 1 mm. from the Heated Surface 51

6. Surface Temperature from Inverse Solution 52

7. Surface Function for the Inverse Test Problem 55

8. Flow Chart (INVRS) 56

9. Assumed Surface Function 61

10. Future Times Versus Time Step Size 64

11. Experimental Model Setup 67

12. Kanthal Wire Heater 68

13. Complete Experimental Setup 69

14. Dresser Basalt Experimental Cylinders 70

15. Temperature Variation with Time for a Typical Dresser Basalt Temperature Test 75

16. Time to Fracture for a Dresser Basalt Cylinder 77

17. Supplemental Fracture Data 79

18. Infinite Cylinder Model 83

19. One-eighth of a Cylinder Model--Four Materials 85

20. Finite Element Grid for One-eighth Cylinder Model 86

21. Plane Model--Two Materials 88

22. Comparison of Surface Temperature for Different Models and One Internal Temperature .. 90

23. Comparison of Surface Temperature Using One Thermocouple and Four Thermocouples 93

24. General Equipment Layout 122

25. General Electrical Block Diagram 123

26. Thermocouple Schematic 124

27. Strain Gage Schematic 125

28. Temperature Gage Schematic 126

LIST OF TABLES

Tables		Page
I	Mechanical Properties Versus Temperature	22
II	Thermocouple Assembly and Air Thermal Properties	87
III	Future Time Versus Time Step Size	89
IV	Time to Fracture	94

NOMENCLATURE AND LIST OF SYMBOLS

The following symbols are used in this presentation.

*, **	- footnote symbol,
$\{\bar{\ }\}$	- column matrix (vector) of dimensions r x 1,
$\{\bar{q}\}$	- sum of heat force vectors,
$\{\bar{q}\}_{ss}$	- steady state thermal load vector,
$\{\bar{q}\}_{t}$	- sum of element heat force vectors at time t,
$\{\bar{q}\}_{t-\Delta t}$	- sum of element heat force vectors at time $t-\Delta t$,
$\{\bar{T}\}_{avg}$	- vector of average nodal point temperatures,
$\{\bar{T}\}_{i}$	- vector of all nodal point temperatures at an intermediate time between t and $t-\Delta t$,
$\{\bar{T}\}_{ss}$	- steady state vector of nodal point temperature,
$\{\bar{T}\}_{t}$	- vector of all nodal point temperatures at time t,
$\{\bar{T}\}_{t-\Delta t}$	- vector of all nodal point temperatures at time $t-\Delta t$,
$[\bar{\ }]$	- matrix of dimensions r x c,
$[\bar{C}]$	- sum of element heat capacity matrices,
$[\bar{C}]_{avg}$	- temperature dependent heat capacity matrix, evaluated at $\{\bar{T}\}_{avg}$,
$[\bar{K}]$	- sum of element conductivity matrices,
$[\bar{K}]_{0}$	- constant conductivity matrix,

$[\overline{\Delta K}]$ - matrix used to adjust thermal loads,

$[\overline{K}]_{avg}$ - temperature dependent conductivity matrix, evaluated at $\{\overline{T}\}_{avg}$,

$[\overline{K}]_{ss}$ - steady state conductive matrix,

$J[\ ]$ - functional,

$J[g]$ - functional in terms of unknown surface function,

r,θ,z - cylindrical coordinates,

x,y,z - cartesian coordinates,

A - beginning time of the measurement of experimental temperature,

a - lower limit of time interval,

B - time at the end of the measurement of the time interval of the experimental temperature,

b - upper limit of time interval,

C - temperature dependent heat capacity,

d - distance from the surface to an internal point,

dg - boundary condition or surface condition improvement,

F_g - partial derivative of F with respect to g,

F_{g_x} - partial derivative of F with respect to g_x,

F_{g_y} - partial derivative of F with respect to g_y,

F_{g_z} - partial derivative of F with respect to g_z,

F_{g_t} - partial derivative of F with respect to g_t,

FEM - Finite Element Method

f(t) - variation of boundary temperature with time,

g - unknown or assumed surface function,

g_0 - starting value of an assumed boundary condition,

g_x - partial derivative of g with respect to x,

g_y - partial derivative of g with respect to y,

g_z - partial derivative of g with respect to z,

g_t - partial derivative of g with respect to t,

h - convective coefficient,

K - temperature dependent conductivity,

K_r - temperature dependent conductivity, evaluated at T_r,

ℓ - iteration parameter for inverse solution,

m - slope of an assumed linear boundary condition

N - number of time steps,

nf - number of future times,

R - region where internal temperatures are known,

R_1 - region where experimental measurements are made,

RMERC - Rock Mechanics and Explosive Research Center at the University of Missouri-Rolla,

r_i - inside radius of a hollow cylinder,

r_0 - outside radius of a hollow cylinder,

r_t - distance from center of hollow cylinder to thermocouple tip,

T - temperature,

T_r - reference temperature,

T_ε - temperature that results from a boundary condition or a surface heat condition of $(g+\varepsilon)$,

Δt - increment of time,

v - iteration index, for iteration of material properties,

V_1, V_2, V_η - small volumes in which temperatures are measured,

W - weighting factor,

Y - given or known experimental temperature,

$\Delta \tau$ - nondimensional interval size,

$\Delta \tau_0$ - time interval size,

ε - small number,

η - index of measured points,

ρ - density,

τ - period variation of surface heat,

τ_0 - material property time lag constant,

Θ - transformed temperature,

ν - wave velocity,

Υ - time for a thermal wave to travel from the surface to an internal point,

ω	- frequency of thermal wave,
$\omega_{surface}$	- highest frequency component of surface heat variation.

I. INTRODUCTION

A. The Need for Thermal Analysis of Rock Materials

In recent years much interest has been generated in thermal weakening, thermal fracturing, and combined thermal-mechanical fracturing of rock materials. All of the above require some knowledge of heat transfer in rock materials. In general rock materials are inhomogeneous, anisotropic and have material properties which are temperature dependent. These facts lead to nonlinear partial differential equations which are used to determine their behavior.

The complexity of rock materials has prevented exact analytical treatment of the heat transfer problems. Simplifying approximations of linear, homogeneous, isotropic materials are normally made. Thus, the influence of the temperature dependence of material properties is usually not included. Patel (1)* included the effect of temperature on Young's modulus and Poisson's ratio in his finite element stress analysis. However, the effect of temperature on the thermal properties was not treated. This dissertation will provide a tool for allowing the effect of temperature on thermal properties to be included in the thermal analysis of rock materials. The last step of

---

*Numbers underlined and in parentheses refer to listings in the bibliography.

including the effect of temperature on fracture analysis will require future work.

The usual problem encountered in conductive heat transfer is one where the boundary conditions are known and information is desired about the region inside the boundary. However, a problem of practical importance arises if the heat transfer conditions are known inside the body and the boundary conditions are not known. The first heat conduction problem being the direct problem of heat conduction and the second being classified as the inverse problem of heat conduction. It is evident that a close relationship exists between the direct problem and the inverse problem since they both must satisfy the same laws of heat transfer.

The solution of heat transfer problems, of course, can be no better than the material properties data used in their analysis. Rock material thermal properties have not been tested and cataloged to the extent that many manufacturing materials have been. The need for thermal analysis of rock materials has caused some work to be done to determine the thermal properties of rocks. The number of rock materials that have been tested is limited and the data available for any particular rock is often incomplete. The heat transfer procedures of this dissertation assume that valid thermal properties are available, as will be the case in the future.

As with the thermal properties, temperature dependent material properties for stress analysis are not available for all rock materials. Data for the temperature dependence of fracture properties of rock materials can at best be called a first approximation.

B. The Direct Method of Heat Transfer for Rock Materials

1. Selection of the Finite Element Method Numerous methods are available for solution of heat conduction problems with temperature dependent material properties (2). For problems with complicated geometry as well as temperature dependent material properties, the number of methods is much smaller, primarily the finite difference method and the finite element method. Solutions of complex nonlinear heat conduction problems by finite differences have become quite advanced. The finite element method has been slower developing along these lines, and in fact, is not presently recommended for use with nonlinear transient problems (3). However, the versatility of finite element programs for handling a variety of problems, ease of application and adaptability for instructional purposes can offset any of its present negative aspects.

The heat transfer studies form an integral part of a thermal stress analysis, thus, the thermal analysis and stress analysis should be compatible. The temperature dependent finite element thermal stress program developed by Patel (1) was coupled with the thermal analysis program

of this research to form a completely temperature dependent thermal stress analysis.

It was on this basis that the finite element method was chosen.

2. The Finite Element Method Reference (4) covers the development of the finite element method and includes applications to heat transfer problems. Chapter nine of reference (5) deals with application of the finite element method to heat transfer. The capability of solving all types of nonlinear heat conduction problems is beyond the scope of this dissertation. Only nonlinear heat conduction problems which allow linearization for small time intervals will be considered. A linear formulation of the finite element method and a procedure for changing material properties between time intervals was used.

While there are many difficulties associated with nonlinear heat transfer in rock materials, rock materials in general have a low diffusivity which insures slow penetration of heat and consequently slow changes in temperature within the body. These slow changes in temperature produce slow changes in material properties and allow linearization of the nonlinear partial differential equation, when considered for short intervals of time. Materials other than rock materials that are only mildly temperature dependent can be treated in the same manner if the material properties are changing slowly.

The finite element method divides the body into geometric elements. The time coordinate is also usually divided into small intervals of time. The thermal loads, either due to heat sources or boundary conditions, should not be so large as to produce large temperature gradients across any element during a time interval. The analysis for a time interval was made with each element having its average material properties for that time interval. To obtain the average material properties required iteration. The boundary conditions were assumed to be constant for each individual time interval but were allowed to vary between time intervals.

C. The Inverse Method of Heat Transfer

1. The Reason for Inverse Problems Since thermal properties are incomplete for many rocks, many of the present thermal studies of rock materials are experimental. The experimental measurement of surface heat flux or surface temperatures is difficult in many cases, e.g. ablation, quenching, etc. The boundary temperatures produced by nonlinear heaters will be found by experimentally measuring internal temperatures and calculating the surface temperatures. This procedure, while useful in rock mechanics, also finds applications in other areas where knowledge of surface temperature is desired, e.g. determination of convective coefficients, calculations of surface temperatures inside a combustion chamber, etc.

2. The Associated Direct Problem Closely related to each inverse problem is a direct problem which is called the associated direct problem. An associated direct problem has the same partial differential equation, initial conditions, geometry and material properties but has specified boundary conditions instead of specified internal conditions. Because of its close relationship to the inverse problem, the associated direct problem can be used to give insight to the difficulties in solution of the inverse problem as well as to study parameters which will influence the inverse solution. The geometry as well as the material properties are the same for both the inverse problem and its associated direct problem. If numerical treatment of the associated direct problem was required for its solution because of geometry or temperature dependent material properties, then solution of the inverse problem would also require numerical treatment. In a direct heat conduction problem, if the mode of heat transfer from outside the region to a surface of the region is radiation, then the boundary condition is nonlinear. The inverse problem can be solved for the unknown boundary condition, as either a surface heat flux or a surface temperature, without regard to the method or mode of heat transfer to the surface from outside the region. Thus, if the unknown boundary condition is nonlinear because of the external mode of heat transfer to the boundary, it can be

replaced by a linear boundary condition.

3. Damping and Delay of Thermal Disturbances In general if an internal temperature is measured and the surface heat transfer condition is to be calculated, this requires the solution of an inverse problem. The reconstruction of a surface heat transfer condition from an experimental temperature history will always contain factors of uncertainty. These uncertainties occur because materials that conduct thermal disturbances also damp and delay the thermal disturbances. A thermal disturbance is either a change in heat flux or temperature that occurs over some interval of time. The term damp means that the magnitude of a thermal disturbance will be decreased as it travels between two points in the material. The damping is a function of the frequency content of the thermal disturbance, material properties and distance from the point of origin of the disturbance. The frequency content of a thermal disturbance is the range of frequencies contained in a Fourier series representation of the thermal disturbance. The higher frequencies will be more heavily damped and the greater the distance from the origin of the disturbance, the greater the disturbance will be damped.

The material between a surface thermal disturbance and an internal point acts as a filter that filters out the higher frequencies. A cut off frequency could be defined as the frequency at which the surface temperature

could vary and not be detected by experimental measurement at a selected internal point. Any surface thermal disturbance of higher frequency than the cut off frequency would not affect the measured data. Frequency components of the surface thermal disturbance above the cut off frequency will not appear in the measured data. The filtering action of the material restricts the frequency content of the measured data, thereby restricting the information available to reconstruct the surface thermal disturbance. In fact, the measured data cannot yield information about the surface temperature frequency content above the cut off frequency.

There are two delay times which must be considered when solving an inverse problem based on experimental data. Actual delay time is the time required for thermal disturbances to propagate from one point to another in an experimental or physical body. This delay will occur, because in a physical system time is required for a disturbance to travel between two points. Mathematical model time delay is the time required for the thermal disturbance to propagate from one point to another in the mathematical model. This delay may be zero in a mathematical model and is zero for heat conduction theories based on Fourier's law. Classical heat conduction is based on Fourier's law of heat conduction. One of the recognized drawbacks to the classical heat conduction theory is that

it predicts that the propagation speed of a thermal disturbance is infinite (6). While this appears disturbing at first glance, the classical theory correlates quite well with the bulk of experimental results.

4. Thermal Waves In (1867), Maxwell (7) obtained an additional term in his derivation of Fourier's law but he discarded it. Cattaneo (8) and others (9-15) later used the following relationship to replace Fourier's law.

$$\dot{q} + \sigma q = -K\sigma \frac{\partial T}{\partial x} \tag{1.1}$$

where

q = heat flux

$\dot{q}$ = rate of change of heat flux with time

$\frac{\partial T}{\partial x}$ = temperature gradient

K = thermal conductivity

$\frac{1}{\sigma} = \tau_0$ (1.2)

= time lag required for a steady state condition in a small volume of material subjected to a thermal gradient, which is the time required for the $\dot{q}$ term to become negligible

Their formulation transforms the heat conduction equation from a parabolic equation into a hyperbolic equation. The resulting propagation speeds of thermal disturbances are finite. A physical interpretation of Equation (1.1) is given by Chester (11). If τ_0 is very small Equation (1.1)

reduces to Fourier's law.

$$q = -K \frac{\partial T}{\partial x} \tag{1.3}$$

Later Gurtin and Pipkin (16) set out a general theory of heat conduction which allowed calculation of the speeds of thermal waves. However, they introduced material property functions which are not readily available. They show Equation (1.1) to be a specialized case of their formulation.

Nunziato (17) developed his own constitutive equation and arrived at a formulation similar to that of Gurtin and Pipkin. Nunziato considered a plane progressive damped thermal wave and calculated the wave speed and attenuation of the wave based on his theory. As in the work of Pipkin and Gurtin, special material properties are defined which are not readily available. However, he did show that the wave speed of the new theory approaches the wave speeds obtained by classical theory as the frequency of the wave approaches zero.

Thus, the classical theory and the newer theories come together for thermal disturbances of low frequencies or surface inputs which are relatively slow. The direct and inverse methods of heat conduction are completely dependent on the heat conduction theory selected for analysis. One should be aware that in some situations the classical heat conduction formulation may be in error and

require use of one of the newer heat conduction theories. The inverse method of Chapter III could be used equally well with any of the heat conduction formulations. However, the direct method of Chapter II is formulated based on classical heat conduction theory.

5. Previous Work Inverse problems have been solved by either extrapolation of internal temperatures to obtain the surface temperature, graphical solution of the inverse problem, using a direct heat conduction solution, or an analytical formulation of the inverse problem (18-35). Some of the inverse solutions had oscillations and instabilities. These instabilities are a result of trying to extract all of the information that is present in an internal history. There must be some point at which all of the information has been obtained and any further attempts to extract information will be fruitless. The objective of an inverse method should be to extract all available information. The inverse methods discussed here will be those which either discovered instabilities or indicated how to treat them.

Stolz (18) was one of the first to deal with the inverse problem in the literature. He formulated the inverse problem as a direct problem and then expressed the solution as an integral equation in terms of the unknown boundary condition. He then numerically inverted the integral equation to obtain the unknown boundary condition.

The numerical inversion procedure required that the internal temperature history as well as the boundary condition be constant for each individual time interval. To make this assumption accurate the time interval size in some cases would have to be very small. He discovered that the time step size in his numerical procedure could not be reduced indefinitely without producing numerical oscillations.

Sparrow et al. (25) solved the inverse problem using Laplace transforms. As with Stolz's method the final solution requires numerical inversion of an integral equation. The internal time history was divided into time intervals for the numerical inversion. If the time intervals were made too small, numerical oscillations would appear in their solution. They estimated the time interval size at which oscillations would occur and outlined a procedure for reducing the oscillations. Their procedure utilized the experimental internal history in advance of the time interval being calculated. They could obtain solutions for small time intervals, however, these solutions were directly tied to a larger time interval.

Beck (31) used nonlinear estimation and iterated with the direct solution to solve an inverse problem with temperature dependent material properties. Iteration of a direct solution requires assuming the unknown boundary condition and solving for the internal temperature. An

improvement on the assumed boundary condition is made based on the error between the calculated internal temperature and the experimental temperature specified in the inverse problem. The nonlinear estimation procedure provides a means to calculate improvements to the assumed boundary condition. For linear problems the nonlinear estimation procedure acts as a linear filter (31) and for the nonlinear problems the estimation procedure acts as a basis for iteration for the solution. The nonlinear estimation procedure required the evaluation of the internal temperature response to a change in boundary conditions and solution of the associated direct problem. Beck used a finite difference formulation for numerical evaluation of both the associated direct problem and the internal temperature response due to a change in the boundary conditions. An improvement to the assumed boundary condition was calculated from the internal temperature response to a change in boundary conditions along with the difference between the finite difference solution of the associated direct problem and the given internal history. The use of the finite difference solution required that the boundary condition and the experimental internal history be divided into small time intervals. The boundary conditions were assumed to be constant for each time interval. To make this assumption accurate, it was necessary to be able to make the time intervals small and still obtain a

stable solution. The internal temperature response to a change in boundary conditions was evaluated by applying a small change to the boundary condition for one time interval and dividing the internal temperature change by the change in the boundary condition. If the time interval was small, then the internal temperature response was also small. If the internal temperature response to an improvement in the boundary condition estimate was too small, the estimation procedure became impossible. Beck defined the nondimensional internal temperature response to a change in surface heat flux as a sensitivity coefficient. The iteration procedure requires a sufficiently large sensitivity coefficient to be stable and the larger the sensitivity coefficient the better the convergence.

Beck considered the surface thermal disturbance for a particular time interval to influence the internal temperature at the time interval the disturbance occurs plus some additional time intervals after the time interval of the surface disturbance. He called the additional time intervals future times. He recognized that for small time interval sizes there was a time delay between a surface thermal disturbance and a maximum temperature response at an internal point. His concern was not for calculation of the time delay but taking advantage of the time delay to simplify and stabilize his numerical procedure. Using a finite difference solution to a direct heat conduction

problem, Beck determined a recommended number of future times for four different time interval sizes. He limits his recommendation to small time interval sizes and to a small number of future times. To increase the magnitude of the internal temperature response in his inverse method, he applied his assumed boundary condition for more than one time interval. The number of additional time intervals were equal to his recommended number of future times. He then solved the inverse problem for the extended time period and used that inverse solution to approximate the inverse solution for the first time interval.

This procedure does not really reduce the time step sizes since one must make an assumption of constant surface heat transfer conditions for a longer period of time than the basic time interval. The amount of error will, of course, depend on how fast the surface condition is changing. If the surface condition is nearly constant for the longer period, then the additional time steps would introduce little error. The smaller time steps would not give additional information about the surface condition but would allow the direct problem to be more accurately modeled. Very small steps may be required in the direct problem to allow linearization of the nonlinear partial differential equation.

If the surface conditions do not allow a constant assumption for the larger interval of time, the surface

condition can be assumed to be a linear function of time over the time period. Beck's formulation shows the constant surface condition to be superior to the linear assumption based on sensitivity coefficients.

The limitation on the time interval size is dependent on the accuracy with which the internal response can be calculated. This accuracy will be dependent on the model and on the computing equipment. Thus, each problem will have its own smallest time interval size. If smaller step sizes are required, then more accurate calculations will also be required.

6. Selection of an Inverse Method The inverse method should be applicable to a large variety of problems i.e., temperature dependent materials, composite materials, as well as three dimensional problems. Of the methods considered in the literature only the analytical formulation of the inverse and iteration of a direct solution have the capabilities of solving complicated geometries. Of these two methods, iteration of a direct solution has the added advantage that techniques for solving direct heat conduction problems have been studied for many years and are relatively advanced. It was for this reason that the method of iteration of a direct solution was chosen.

The solution to an inverse problem by iteration with a direct solution requires only the ability to solve the direct problem for an assumed surface condition and a

method of improving the assumed surface condition. The procedure involves assuming a surface condition and using the direct method to solve for the internal temperatures. The calculated internal temperatures are compared to the given internal temperatures to check the validity of the assumed surface condition. If the assumed surface condition is in error, then an improvement is made to the assumed surface condition. The iteration is continued until an acceptable surface condition is obtained.

The inverse method of this research will be based on the principles outlined by Beck (31), however, a more general variational approach is taken to determine the surface heat function. Beck's formulation is then a special case of the more general formulation of this research. It will be shown here that the estimate of the delay time can be used to stabilize the numerical procedure.

7. Experimental Example A practical test requires the use of the inverse method with experimental data. During the course of this research, experimental data was collected on heat transfer from Kanthal wire wound heaters to hollow Dresser Basalt cylinders. The modes of heat transfer were radiation, conduction and convection from the heater to the inside surface of the Dresser Basalt cylinder. These experiments were to give insight into heat transfer from the heaters to Dresser Basalt for use in thermal stress and thermal fracture studies.

Since the Dresser Basalt cylinders of the experiments would fracture during their thermal test, they were also instrumented with strain gages. Thus, the tests would provide heat transfer data as well as fracture data. The inverse solution which resulted from experimental data was used with the direct method to obtain internal temperature distributions. Thermal stresses were calculated, as well as time to fracture, for a simple infinite cylinder model. The time to fracture for the simple model was compared to that of the experimental model.

D. Discussion of Fracture Considerations

A full discussion of fracture analysis is beyond the scope of this dissertation, however, a few brief remarks will be made. Tettleman (36) states, "Fracture is an inhomogeneous process of deformation that causes regions of material to separate and load carrying capacity to decrease to zero."

It is obvious from this definition that fracture is a highly localized condition. The formation of a crack will depend on local conditions at the tip of the crack. The difficulty in predicting under what condition a crack will form is evidenced by the number of papers in the literature dealing with fracture. The extension of the theory of fracture from a localized condition to a crack propagating across an arbitrarily loaded and arbitrarily

shaped body adds another dimension to the problem.

Jaeger (37) discusses many aspects of fracture of rock materials including four fracture theories and seven types of fracture tests, as well as some of the many things that complicate the analysis of fracture of rock materials. The four theories discussed by Jaeger are the Coulomb-Navier theory, the Mohr theory, the Griffith theory, and the modified Griffith theory. All of these fracture theories predict tensile fracture initiation when the tensile stress is greater than the tensile fracture stress of a specimen in a tensile test. One of the theories to predict fracture initiation in rock materials is the criteria for fracture initiation as developed by Griffith and modified by McClintock-Walsh (38).

The modified Griffith criteria is used to predict fracture initiation if the stress normal to the crack tends to cause crack closure. If the stress normal to the crack is tensile, the original Griffith criteria is used to predict fracture initiation. When the tensile stresses in a brittle rock material at a crack tip reach a critical value, then fracture initiation, fracture propagation and complete failure can occur nearly simultaneously. For tensile stresses, Griffith's fracture initiation criterion may be used to predict the strength behavior of rock (39).

The problem becomes further complicated when the stresses are thermally induced. Chen and Marovelli (40)

state, "Although the number of published analytical and experimental investigations conducted on ceramic and refractory materials is large, the literature reveals there is a lack of information on both the theoretical and actual response of rock to thermal shock."

The Griffith criteria although not specifically formulated for predicting thermal fracture initiation in an arbitrarily shaped rock body can be used as a first approximation to thermal fracture initiation. For an infinite hollow cylinder with only a radial temperature variation resulting from internal heating, the fracture criteria are satisfied when the tangential stress is greater than the tensile fracture stress.

E. Material Properties

Few if any natural rock materials have all of their thermal or mechanical properties available for a complete temperature, thermal stress or fracture analysis. There is no universal set of units for the thermal properties and no data to indicate how temperature affects fracture strength. Dresser Basalt has been a popular material for thermal stress studies because it does have many of its thermal and mechanical properties tabulated. Dresser Basalt was chosen for the experimental tests of this dissertation. The units of the material properties are given as they appear in the literature. Finite element programs

are normally written for a consistent set of dimensional units throughout. After the FEM programs of this research were checked by solving example problems, then the necessary changes were made to copies of the program to allow the dimensional units to be mixed. These altered programs converted dimensional units, where necessary, and were designated as "special".

Dresser Basalt is considered as a relatively homogeneous material. The properties are as follows:

1. Heat capacity (41) is given as a bilinear curve as

$C_p = C_0 + C_1 T$ $\quad 100°C \leq T \leq 575°C$

$C_0 = 0.217579$

$C_1 = 0.123421 \times 10^{-3}$

$C_p = 0.258507$ $\quad 575°C \leq T \leq 1000°C$

C_p = heat capacity, $(\frac{cal}{gram°C})$

T = temperature, degrees Centigrade

There is no data given for the heat capacity below 100°C and the heat capacity is discontinuous at 575°C. For the purposes of this research the heat capacity curve was extrapolated to include temperatures down to 20°C.

2. Thermal conductivity (42) is given as

$1/K = K^1_0 + K^1_1 T + K^1_2 T^2 + K^1_3 T^2$ $\quad 500°R < T \leq 2100°R$

$K^1_0 = 0.6272$

$K^1_1 = 2.965 \times 10^{-4}$

$K^1_2 = -2.067 \times 10^{-7}$

$K^1_3 = 9.327 \times 10^{-11}$

K = thermal conductivity, $(\frac{\text{Btu}}{\text{ft hr °F}})$

T = temperature, degrees Rankine

3. Density is considered constant and is given as 2.97 gm/cm^3 (43).

4. The convective coefficient, h, is approximated as 0.00021 cal/cm^2-sec-°C (1, 44, 45, 46).

5. The values of the Poisson's ratio, Young's modulus and the coefficient of thermal expansion are given in Table I (43).

TABLE I

Mechanical Properties Versus Temperature

T, degrees Centigrade	E, 10^9 N/M	μ	$\alpha T \times 10^{-2}$
24	100.7	.24	0.007
122	98.6	.24	0.140
260	95.1	.22	0.200
371	87.6	.19	0.350

where

E = Young's modulus

μ = Poisson's ratio

α = thermal expansion coefficient

6. The ultimate strength in tension of Dresser Basalt is given as 2,195 psi (1).

7. The influence of temperature on fracture strength is not available.

F. Influence of Thermocouples on Measured Temperature

Temperatures measured in materials with low conductivities can be considerably in error when measured by a thermocouple with a much higher conductivity. Beck (47-49) shows that the removal of material for subsurface temperature measurement, as well as differences between material properties of the thermocouple and measured material can introduce considerable error in temperature measurements. These errors can be approximately accounted for when solving the inverse method by including the thermocouple in the mathematical model of the experiment.

G. Objective and Scope

The object of this dissertation is to develop and demonstrate a practical method for the study of heat transfer in rock materials both from direct and inverse considerations.

The scope of this thesis is:

1. The development of an analysis technique to evaluate temperature distributions in rock materials. The rock materials may have temperature dependent material properties but these functions must be continuous functions

as well as have continuous first derivatives with respect to temperature.

2. The development of an analysis technique to solve for surface temperatures or surface heat fluxes from experimentally measured internal temperatures.

3. Experimental measurement of internal temperatures for Dresser Basalt cylinders.

4. Experimental measurement of time to fracture for Dresser Basalt cylinders.

5. Simplified stress and fracture analysis to indicate possible use of the heat transfer programs.

II. THE DIRECT METHOD

A linear transient finite element thermal analysis was used to approximate temperature distributions in materials with temperature dependent properties. The material properties were assumed to be constant for any one time interval but were allowed to vary between time intervals. The element material properties were based on the average temperature of the element for each time interval. Iteration was required to obtain the element average temperature.

A. Linear Finite Element Equations

The finite element matrix form of the linear transient heat conduction equation given by Wilson and Nickell (50) is

$$([\bar{C}] + \frac{1}{2}\Delta t[\bar{K}])\{\bar{T}\}_t = ([\bar{C}] - \frac{1}{2}\Delta t[\bar{K}])\{\bar{T}\}_{t-\Delta t} + \frac{1}{2}\Delta t\{\bar{q}\}_t + \frac{1}{2}\Delta t\{\bar{q}\}_{t-\Delta t} \quad (2.1)$$

where

$[\bar{K}]$ = sum of element conductivity matrices

$[\bar{C}]$ = sum of element heat capacity matrices

$\{\bar{q}\}_t$ = sum of element heat force vectors at time t

$\{\bar{q}\}_{t-\Delta t}$ = sum of element heat force vectors at time $t-\Delta t$

$\{\bar{T}\}_t$ = vector of all nodal temperatures at time t

$\{\bar{T}\}_{t-\Delta t}$ = vector of all nodal temperatures at time $t-\Delta t$

To simplify the solution they define a new vector of nodal temperature as

$$\{\bar{T}\}_i = \frac{1}{2}\{\bar{T}\}_t + \frac{1}{2}\{\bar{T}\}_{t-\Delta t} \tag{2.2}$$

Substituting Equation (2.2) into Equation (2.1) and re-arranging gives

$$(\frac{2}{\Delta t}[\bar{C}] + [\bar{K}])\ \{\bar{T}\}_i = \frac{2}{\Delta t}[\bar{C}]\ \{\bar{T}\}_{t-\Delta t} + \frac{1}{2}\{\bar{q}\}_t + \frac{1}{2}\{\bar{q}\}_{t-\Delta t} \tag{2.3}$$

The only unknown in Equation (2.3) is the temperature vector $\{\bar{T}\}_i$.

B. Linear Approximation for the Nonlinear Case

The linear approximation consists of assuming the material properties to be constant for each time interval and equal to the average properties for that time step. Using average material properties in Equation (2.3) gives

$$(\frac{2}{\Delta t}[\bar{C}]_{avg} + [\bar{K}]_{avg})\{\bar{T}\}_i = \frac{2}{\Delta t}[\bar{C}]_{avg}\{\bar{T}\}_{t-\Delta t} + \frac{1}{2}\{\bar{q}\}_t + \frac{1}{2}\{\bar{q}\}_{t-\Delta t} \tag{2.4}$$

where

$$\{\bar{T}\}_{avg} = \frac{\{\bar{T}\}_t + \{\bar{T}\}_{t-\Delta t}}{2} \tag{2.5}$$

$\{\bar{T}\}_{avg}$ = vector of average nodal temperatures

$[\bar{C}]_{avg}$ = temperature dependent heat capacity matrix, evaluated at $\{\bar{T}\}_{avg}$

$[\bar{K}]_{avg}$ = temperature dependent conductivity matrix, evaluated at $\{\bar{T}\}_{avg}$

The average material properties for each time step are found by iteration. Equation (2.4) was solved by using the following iteration equation.

$$\left(\frac{2}{\Delta t}[\bar{C}]^{v}_{avg} + [\bar{K}]^{v}_{avg}\right)\{\bar{T}\}^{v+1}_{i} = \frac{2}{\Delta t}[\bar{C}]^{v}_{avg}\{\bar{T}\}_{t-\Delta t} + \frac{1}{2}\{\bar{q}\}_{t} + \frac{1}{2}\{\bar{q}\}_{t-\Delta t} \qquad (2.6)$$

where

v = iteration index

The first step of the procedure is to assume $\{\bar{T}\}^{v}_{t}$ and evaluate the material properties based on an average temperature $\{\bar{T}\}^{v}_{avg}$ where

$$\{\bar{T}\}^{v}_{avg} = \frac{\{\bar{T}\}^{v}_{t} + \{\bar{T}\}_{t-\Delta t}}{2} \qquad (2.7)$$

Then solve Equation (2.6) for $\{\bar{T}\}^{v+1}_{i}$.

If the difference between $\{\bar{T}\}^{v+1}_{i}$ and $\{\bar{T}\}^{v}_{i}$ is small, then the iteration procedure is completed. If the difference is too large, then $\{\bar{T}\}^{v}_{i}$ is set equal to $\{\bar{T}\}^{v+1}_{i}$ and the iteration is started again.

C. Comparison of a Linearized Finite Element Method Solution to Kirchoff Transformations

One method of solving heat conduction problems with temperature dependent material properties is the Kirchoff transformation (51). Kirchoff's transformation is

$$\Theta = \frac{1}{K_r} \int_{T_r}^{T} K(u)\ du \qquad (2.8)$$

where

$K_r = K(T_r)$

T_r = reference temperature

Θ = transformed variable

The Kirchoff transformation can change a nonlinear partial differential equation in terms of T into a linear partial differential equation in term of Θ.

To test the linearized finite element method, a nonlinear example problem was solved by the linearized finite element method and then solved using Kirchoff's transformation. The Kirchoff transformation was applied to the example problem changing it to a linear problem, then solving it using a linear finite element program.

1. Nonlinear Example Problem An infinite hollow cylinder initially at 20°C had its inside surface raised to 100°C at a time equal to zero. The outside surface was held at 20°C. The inside radius was 1.27 cm. and the

outside radius was 5.08 cm. The partial differential equation is

$$\frac{1}{r}\frac{\partial}{\partial r}\left[K(T)\ r\ \frac{\partial T}{\partial r}\right] = \rho C(T)\ \frac{\partial T}{\partial t} \tag{2.9}$$

The boundary and initial conditions were

$$T(r_i,t) = 100.0°C \qquad t > 0 \tag{2.10}$$

$$T(r_0,t) = 20.0°C \tag{2.11}$$

$$T(r,0) = 20.0°C \qquad t = 0 \tag{2.12}$$

The material properties were

$$K(T) = .1T \tag{2.13}$$

= conductivity

$$C(T) = .1T \tag{2.14}$$

= heat capacity

$$\rho = 1.0 \tag{2.15}$$

= density

$$r_i = 1.27 \tag{2.16}$$

= inside radius

$$r_0 = 5.08 \tag{2.17}$$

= outside radius

2. Transformed Example The transformed partial differential equation is

$$\frac{1}{r}\frac{\partial}{\partial r}\left(r\ \frac{\partial \Theta}{\partial r}\right) = \rho\frac{C(T)}{K(T)}\ \frac{\partial \Theta}{\partial t} \tag{2.18}$$

The reference temperature was 20°C and resulting transformed boundary and initial conditions are

$$\Theta(r_i,t) = 480 \qquad t > 0 \qquad (2.19)$$

$$\Theta(r_o,t) = 0.0 \qquad (2.20)$$

$$\Theta(r,0) = 0.0 \qquad t = 0 \qquad (2.21)$$

To transform back to temperature

$$T = \sqrt{20\Theta + 400} \qquad (2.22)$$

3. Comparison The largest differences between the solutions of the two methods were encountered at the earliest times. As the time increased the differences were reduced considerably. Figure 1 shows the temperature distributions across the cylinder for time equal to .05 sec. from the nonlinear finite element solution and from the Kirchoff transformation solution.

The use of the finite element method for solution of the Kirchoff transformation problem makes the accuracy of its solution dependent on time interval size. As would be expected the smaller the time step, the closer the two solutions were to each other. Figure 2 shows the convergence of the solution of the two methods for the temperature at a particular point in the cylinder.

D. Steady State Analysis

For a steady state analysis, Equation (2.6) reduces to

$$[\bar{K}]^{v}_{avg} \{\bar{T}\}^{v+1}_{i} = \{\bar{q}\}_{t} \qquad (2.23)$$

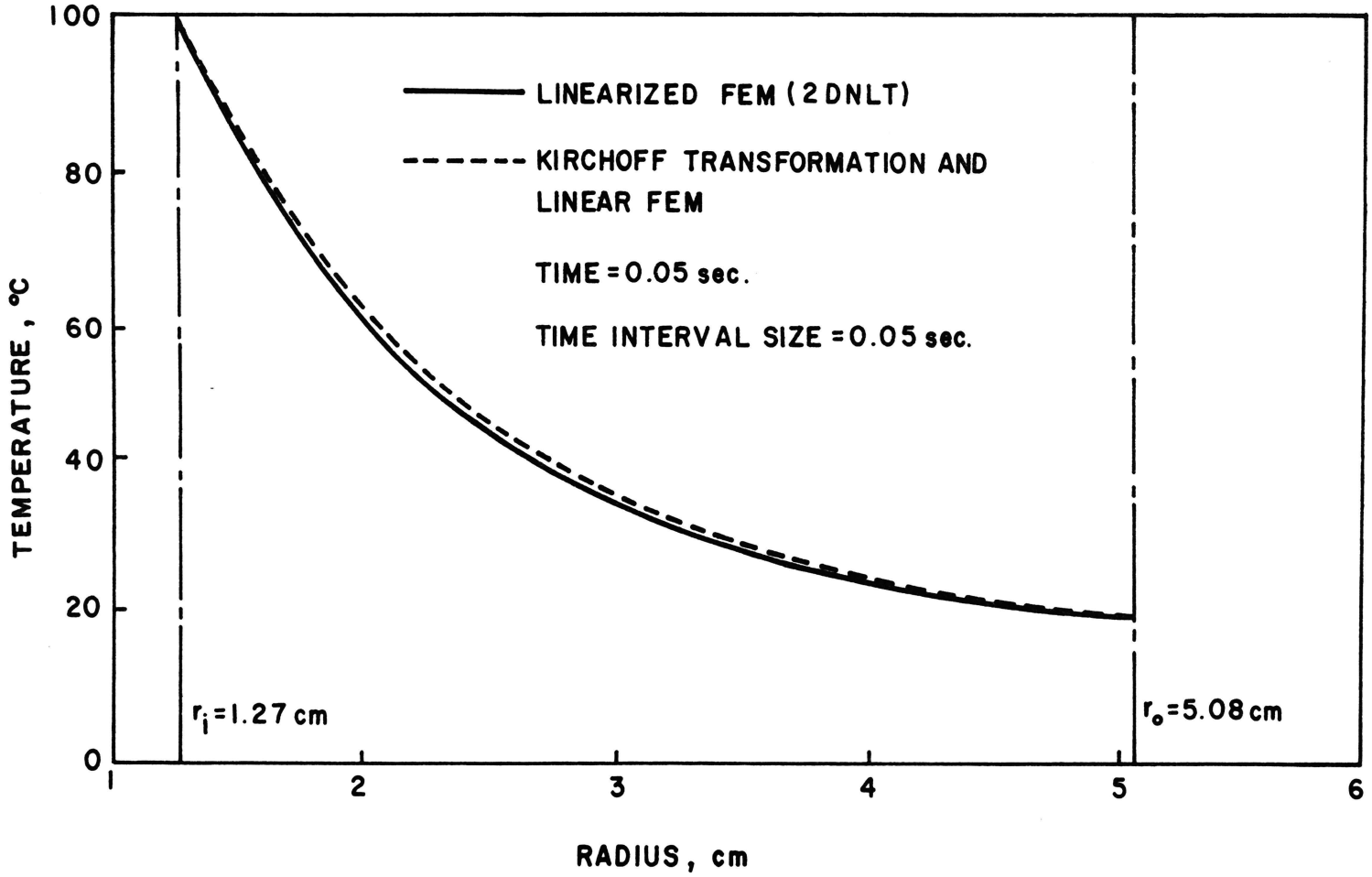

Figure 1 Comparison of Linearized Finite Element Program (2DNLT) Solution with Kirchoff Transformation Solution

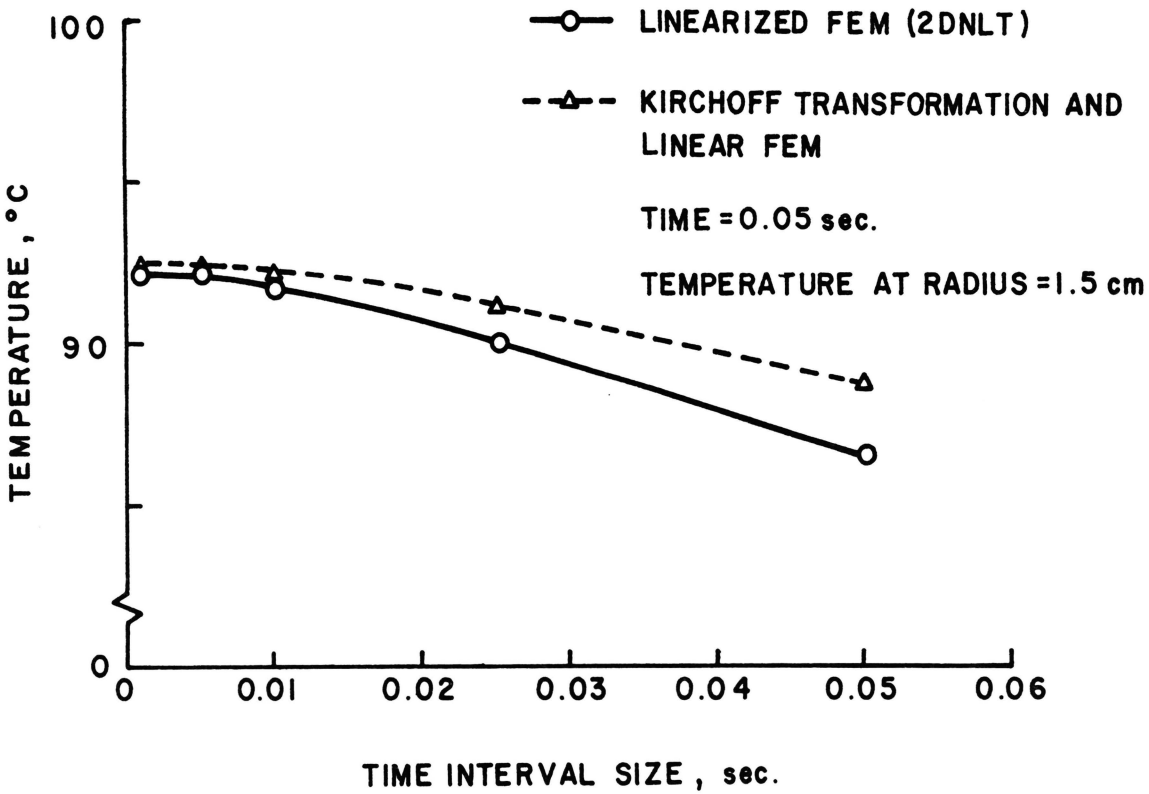

Figure 2 Convergence of Linearized Finite Element Program (2DNLT) Solution and Convergence of Kirchoff Transformation Solution

It should be noted that the average conductivity matrix is based on a short time step near steady state so the average conductivity would be essentially the steady state conductivity, or

$$[\bar{K}]_{ss} \{\bar{T}\}_{ss} = \{\bar{q}\}_{ss} \tag{2.24}$$

where

$\{\bar{q}\}_{ss}$ = steady state thermal load vector

$[\bar{K}]_{ss}$ = steady state conductivity matrix

$\{\bar{T}\}_{ss}$ = steady state nodal temperatures

The iteration procedure is

$$[\bar{K}]^{v} \{\bar{T}\}^{v+1} = \{\bar{q}\}_{ss} \tag{2.25}$$

This procedure requires the reformulation of the conductivity matrix for each iteration.

E. Alternate Steady State Procedure

An alternate iteration procedure for steady state is obtained by defining the steady state conductivity matrix as

$$[\bar{K}]_{ss} = [\bar{K}]_{0} + [\Delta \bar{K}] \tag{2.26}$$

where

$[\bar{K}]_{0}$ = a constant conductivity matrix

$[\Delta \bar{K}]$ = the necessary matrix to make Equation (2.26) correct

This procedure allows the conductivity matrix $[\bar{K}]_0$ to remain constant and $[\Delta\bar{K}]$ to be adjusted to satisfy Equation (2.25). The iteration equation is

$$[\bar{K}]_0 \{\bar{T}\}^{v+1} = \{\bar{q}\}_{ss} - [\Delta\bar{K}]^v \{\bar{T}\}^v \qquad (2.27)$$

The advantage of this procedure is that the conductivity matrix does not have to be reformulated. The above procedure was investigated because less work is required per iteration. However, the total number of iterations was higher using the alternate method. The result was that the alternate method was slower than the previous method. For this reason the alternate method was discarded.

An iteration acceleration method that may be useful for reducing the number of iterations required was developed by Boyle and Jennings (52). This procedure was encountered too late for use in this dissertation.

F. Finite Element Program

A finite element program based on the formulation given by Wilson and Nickell (50) was modified to allow temperature dependent material properties. The original program is proprietary and details cannot be given here (53). However, the method of modification is relatively simple and can be readily applied to any available finite element program. A flow chart indicating the modification procedure is given in Figure 3. The modified program is

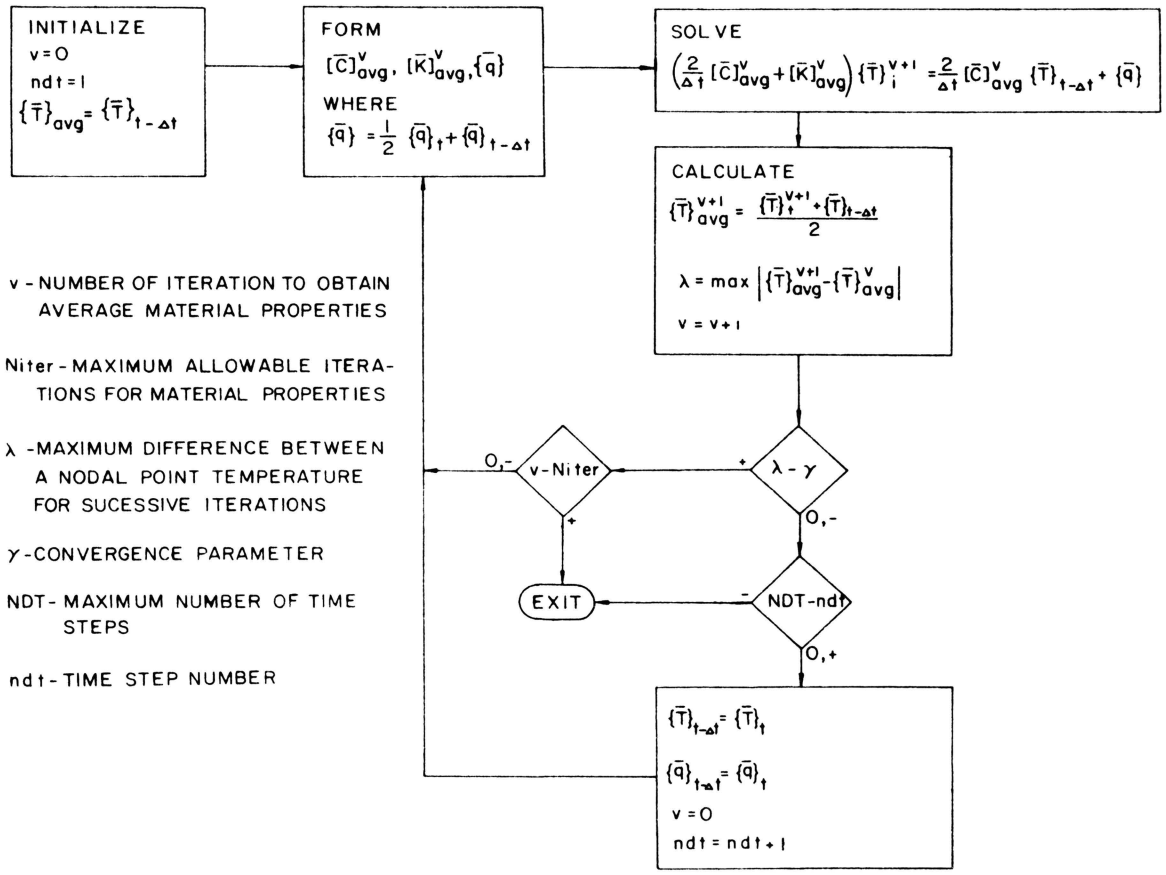

Figure 3 Flow Chart (2DNLT)

called "2DNLT" and is presently being used for research in the RMERC. Input instructions for 2DNLT are included in Appendix A.

III. THE INVERSE METHOD OF HEAT CONDUCTION

The solution of the inverse problem of this research is obtained by iteration of a direct problem. Starting with a direct problem, a boundary condition is found that can be used with the direct problem to calculate an internal temperature history equal to the given experimental internal history. The cases where an exact solution to an inverse problem can be obtained are limited and some error will exist in the solution of most inverse problems. Since an exact solution is not always possible, a criteria for an acceptable inverse solution in this dissertation is as follows:

> An acceptable solution to the inverse problem is the boundary condition which minimizes the least squared error between the given experimental internal temperature history and an internal history obtained from solution of the direct problem.

A. Mathematical Formulation of the Inverse Problem for Solution by Iteration of a Direct Solution

The error in a least squares sense between calculated internal temperatures and given experimental internal temperatures over the time interval $A \leq t \leq B$ and region R can be expressed as a functional.

$$J\left[g\right] = \int_A^B \int_R (T-Y)^2 dx\, dy\, dz\, dt \tag{3.1}$$

where

$$T = T(x,y,z,t,g) \tag{3.2}$$

= internal temperature resulting from the assumed boundary condition

$$g = g(t) \tag{3.3}$$

= assumed boundary condition

$$Y = Y(x,y,z,t) \tag{3.4}$$

= given or known experimental temperature

R = region where internal temperatures are known

A = earliest time the internal temperature is recorded

B = end of the time interval the internal temperature is recorded

Minimizing $J\left[g\right]$ with respect to g will insure the criterion for an acceptable solution is satisfied. To minimize $J\left[g\right]$ the Euler-Lagrange Differential Equation (54) must be satisfied, or

$$F_g - \frac{\partial}{\partial x} F_{g_x} - \frac{\partial}{\partial y} F_{g_y} - \frac{\partial}{\partial z} F_{g_z} - \frac{\partial}{\partial t} F_{g_t} = 0 \tag{3.5}$$

where

$$F = (T-Y)^2 \tag{3.6}$$

$$F_g = \frac{\partial F}{\partial g} \tag{3.7}$$

$$= 2(T-Y)\frac{\partial T}{\partial g} \tag{3.8}$$

$$F_{g_x} = \frac{\partial F}{\partial(\frac{\partial g}{\partial x})} \tag{3.9}$$

$$F_{g_y} = \frac{\partial F}{\partial(\frac{\partial g}{\partial y})} \tag{3.10}$$

$$F_{g_z} = \frac{\partial F}{\partial(\frac{\partial g}{\partial z})} \tag{3.11}$$

$$F_{g_t} = \frac{\partial F}{\partial(\frac{\partial g}{\partial t})} \tag{3.12}$$

$$F_{g_x} = F_{g_y} = F_{g_z} = F_{g_t} = 0 \tag{3.13}$$

Equation (3.5) can be rewritten as

$$2(T-Y)\ \frac{\partial T}{\partial g} = 0 \tag{3.14}$$

More than one internal temperature may be experimentally recorded or measured at many points in a region. When selecting the number of experimental internal temperatures, one should consider the relative importance of the measurements and the desired weighting factor for each measurement. If they all were equally accurate and had similar frequency content, then the primary consideration would be the area or volume of material one had information about. Another important consideration in the procedure would be the distance of the measured point from the original thermal disturbance. The greater the distance the smaller the amount of information an internal temperature history will contain. The simplest way to include

all measured points and allow each to be weighted is to integrate* over the measured region.

$$\int_{R_1} W(T-Y) \frac{\partial T}{\partial g} \, dx \, dy \, dz = 0 \qquad (3.15)$$

where

$$W = W(x,y,z) \qquad (3.16)$$

= weighting factor

R_1 = region of experimental measurements

Some direct problems cannot be solved such that the internal temperature and internal response to a surface condition change can be written explicitly. If a numerical procedure is required for evaluation of the direct problem where the time dimension is subdivided into small intervals, then Equation (3.14) can be applied so it is satisfied over each of the smaller intervals. This is achieved by integration over each of the smaller time intervals.

$$\int_a^b \int_{R_1} W(T-Y) \frac{\partial T}{\partial g} \, dx \, dy \, dz \, dt = 0 \qquad (3.17)$$

where

a = lower limit of time interval

---

*requires average error to be zero but does not minimize the least squares error

b = upper limit of time interval

The closer a measurement is made to the surface, the more information the measurement will contain because the internal temperature history will have a larger frequency content. It is reasonable to assume that if multiple temperature measurements are made, they would be made as close to the surface as possible and at equal distances from the surface. For multiple measurements at equal distances from the surface, the weighting factor would not be necessary and Equation (3.17) could be expressed as

$$\int_a^b \int_{R_1} (T-Y) \frac{\partial T}{\partial g} \, dx \, dy \, dz \, dt = 0 \qquad (3.18)$$

If T, Y and $(\partial T/\partial g)$ are assumed to be constant over small areas or volumes and then integrating Equation (3.18)

$$\int_a^b \Big((T_1-Y_1) \frac{\partial T_1}{\partial g} V + (T_2-Y_2) \frac{\partial T_2}{\partial g} V_2 + \cdots + (T_\eta-Y_\eta) \frac{\partial T_\eta}{\partial g} V_\eta \Big) \, dt = 0 \qquad (3.19)$$

where

V_η = volume in which the temperatures are specified

η = index of the measured points

For simplicity assume that Y is known over only one small area, then Equation (3.19) reduces to

$$\int_a^b (T-Y)\ \frac{\partial T}{\partial g}\ dt = 0 \qquad (3.20)$$

Equation (3.20) is a mathematical statement that will insure that the criteria for an acceptable solution is satisfied. The direct problem provides a relationship between the assumed boundary condition and the internal temperature. An additional equation is needed which relates the internal temperature to an improvement in the assumed boundary condition.

Expressing the internal temperature as the first two terms of a Taylor's series

$$T^{\ell+1} = T^{\ell} + \frac{\partial T^{\ell}}{\partial g}\ dg^{\ell} \qquad (3.21)$$

where

dg^{ℓ} = a boundary condition improvement

Equation (3.21) provides the needed relationship between an improvement in the assumed boundary condition and the internal temperature. It should be recognized that dg is an increment of g and like g may be a function of time, or

$$dg^{\ell} = dg^{\ell}\ (t) \qquad (3.22)$$

Substituting Equation (3.21) into Equation (3.20) gives

$$\int_a^b (T^{\ell} + \frac{\partial T^{\ell}}{\partial g}\ dg^{\ell} - Y)\ \frac{\partial T^{\ell}}{\partial g}\ dt = 0 \qquad (3.23)$$

or

$$\int_a^b \left(\frac{\partial T^{\ell}}{\partial g}\right)^2 dg^{\ell}\, dt = \int_a^b (Y-T^{\ell}) \frac{\partial T^{\ell}}{\partial g}\, dt \qquad (3.24)$$

Equation (3.24) combines the criteria for an acceptable inverse solution with an improvement to an assumed inverse solution.

B. Evaluation of Improvement dg

The easiest assumption for dg is that it is a constant. This assumption allows direct integration of Equation (3.24).

$$dg = \frac{\int_a^b (Y-T^{\ell}) \frac{\partial T^{\ell}}{\partial g}\, dt}{\int_a^b \left(\frac{\partial T^{\ell}}{\partial g}\right)^2 dt} \qquad (3.25)$$

The numerical evaluation of the response ($\partial T/\partial g$) is also very easy. A small change is made in g and the change in T is calculated with the direct method. Although a constant dg is the easiest assumption, there may be times when a more complicated assumption for dg would be useful. Appendix B contains evaluations of Equation (3.24) for four other assumed forms of dg.

The evaluation of dg will also depend on the assumed form of the surface function or boundary condition g.

1. Constant Surface Condition g For a constant g assumption, the evaluation of dg is particularly simple. The direct solution is used to find the internal temperatures for the assumed value of g. Then g is changed by a constant value and the internal temperatures are found for the (g+ε) surface or boundary condition. Then $(\partial T/\partial g)$ is approximated by

$$\frac{\partial T}{\partial g} \simeq \frac{T-T_\varepsilon}{\varepsilon} \qquad (3.26)$$

where

T_ε = internal temperature obtained from assumed g plus ε

ε = small number

2. Linear Surface Condition g A linear assumption for g could be expressed as

$$g^\ell = g_0^\ell + m(t-a) \qquad a \leq t \leq b \qquad (3.27)$$

where

g_0 = starting value of assumed boundary condition g(t)

m = slope of assumed boundary with time

a = time at the start of the time interval

b = time at the end of the time interval

If a linear g is assumed, a constant dg implies a change of g by a constant factor of dg. The result of a constant dg would be a new linear g with the same slope m as the

previous g and a new value of g_0. The final solution for g would then have the same slope m as the original assumption of g. If the slope of g is known before starting the iteration, then the procedure for solution is exactly as in paragraph 1, except for the constant g being replaced with a linear g.

In general the slope of g will not be known before the solution of the inverse is obtained. Usually the value of g will be known at the start of the interval and not at the end of the interval. An iteration procedure should allow the slope of the surface function to be changed during an iteration. One method which would allow the slope of g to change would be to make dg a linear function of time and reevaluate Equation (3.24). Another method is to solve for a constant dg as previously indicated, then apply dg to g as follows

$$g^{\ell+1} = g_0 + m^{\ell+1}\,(t-a) \qquad a \leq t \leq b \tag{3.28}$$

where

$$\begin{aligned} g_0 &= \text{starting interval surface condition} \\ m^{\ell+1} &= m^{\ell} + dg^{\ell} \end{aligned} \tag{3.29}$$

C. Iteration Solution

If the inverse problem is linear and g is constant for the time interval, then only one value of dg must be found. However, if g is not constant or if the inverse

problem is nonlinear, then iteration will be required to find g.

Equation (3.24) forms the basis of iteration for the surface heat function. The procedure is as follows:

1. Assume the function g^{ℓ} for the time interval $a \leq t \leq b$.

2. Solve the direct heat conduction problem for T^{ℓ} and if possible evaluate $(\partial T/\partial g)$. It may not be possible to write $(\partial T/\partial g)$ explicitly from the direct solution, but $(\partial T/\partial g)$ may have to be evaluated numerically.

3. Solve Equation (3.24) for dg^{ℓ} and check the increment dg^{ℓ} to see if it is small over the time interval

$$\text{Maximum } |dg^{\ell}| \leq \varepsilon \qquad a \leq t \leq b \tag{3.30}$$

where ε is a small number and Maximum $|dg^{\ell}|$ is the maximum absolute value of the increment dg over the time interval $a \leq t \leq b$.

4. If dg^{ℓ} satisfies Equation (3.30) stop the iteration, if not continue to step 5.

5. Let

$$g^{\ell+1} = g^{\ell} + dg^{\ell} \tag{3.31}$$

Set

$$g^{\ell} = g^{\ell+1} \tag{3.32}$$

and calculate new values of T^{ℓ} and $(\partial T/\partial g)$. Repeat steps three through four.

When a solution is to be obtained by iteration, the stability of the iteration is an important consideration. The solution of the inverse problem by iteration of a direct solution can be only as stable as the direct solution. As can be seen in Equation (3.24), another factor which will influence the stability of the solution is the internal response $(\partial T/\partial g)$. As long as the response $(\partial T/\partial g)$ of the internal point is of sufficient magnitude to evaluate Equation (3.24), then the stability of the solution will depend on the stability of the direct solution. If the response $(\partial T/\partial g)$ is very small, then the stability of the inverse solution also depends on how accurately the response can be calculated.

As the time interval is reduced in size the magnitude of the response $(\partial T/\partial g)$ is also reduced. If the time interval is too small, then the internal response may become too small to evaluate the internal response $(\partial T/\partial g)$ of Equation (3.24).

A method of overcoming this problem is to solve the inverse for more time intervals so the magnitude of the internal response $(\partial T/\partial g)$ is large enough to allow a stable solution of Equation (3.24). The solution for the extended time period is then used to approximate the inverse solution for the first time interval. The additional time

intervals used in the solution were called future times. This procedure requires an assumption of how the surface function varies over the enlarged interval. If the assumption is not similar to the true surface function, some error will be introduced. The first assumption would be that the surface function is constant over the additional intervals. After solving the inverse problem, the validity of the constant surface condition assumption can be verified. Another procedure is to assume that the boundary condition or surface function is linear over the time interval.

D. Particular Examples of the Inverse Method

The data or experimental internal temperature history of the inverse examples was generated by the finite element method of Chapter II from the equivalent direct problem. The first example has a large change in surface temperature which results in large variations in material properties. The second example is an arbitrarily selected curve. The geometry of both examples is an infinite hollow cylinder with an inside radius of 1.27 cm. and an outside radius of 5.08 cm. The finite element model of the cylinder was made up of forty elements of equal size.

Example 1

The boundary and initial conditions for the direct problem are

$$T(r_i,t) = 1250°C \qquad t > 0 \tag{3.33}$$

$$-K(T)\frac{\partial T}{\partial r}(r_0,t) = h\left(T(r_0,t) - T_\infty\right) \tag{3.34}$$

$$T_\infty = 20°C \tag{3.35}$$

$$T(r,t) = 20°C \qquad t \leq 0 \tag{3.36}$$

$$r_i = 1.27 \text{ cm.} \tag{3.37}$$

$$r_0 = 5.08 \text{ cm.} \tag{3.38}$$

The material is Dresser Basalt.

An internal temperature history was generated using the direct program that is discussed in Chapter II. Figure 4 shows the temperature distribution across the cylinder at .05 seconds. The temperature history at 1 mm. from the heat surface is given for three different time step sizes in Figure 5. The temperature history is nearly equal for all of the time steps. A time step of .05 seconds was used to solve for the surface temperature and the results are shown in Figure 6.

The boundary condition of Equation (3.33) is a step change in the surface temperature which occurs instantaneously. This condition is, of course, a physical impossibility because some time is required to change the surface temperature. The direct method was set up to allow the type of boundary condition of Equation (3.33). When solving the direct method with a step surface temperature change, the material properties are based on the average element temperature for each time step. The first time interval, thus, includes the step change in surface tem-

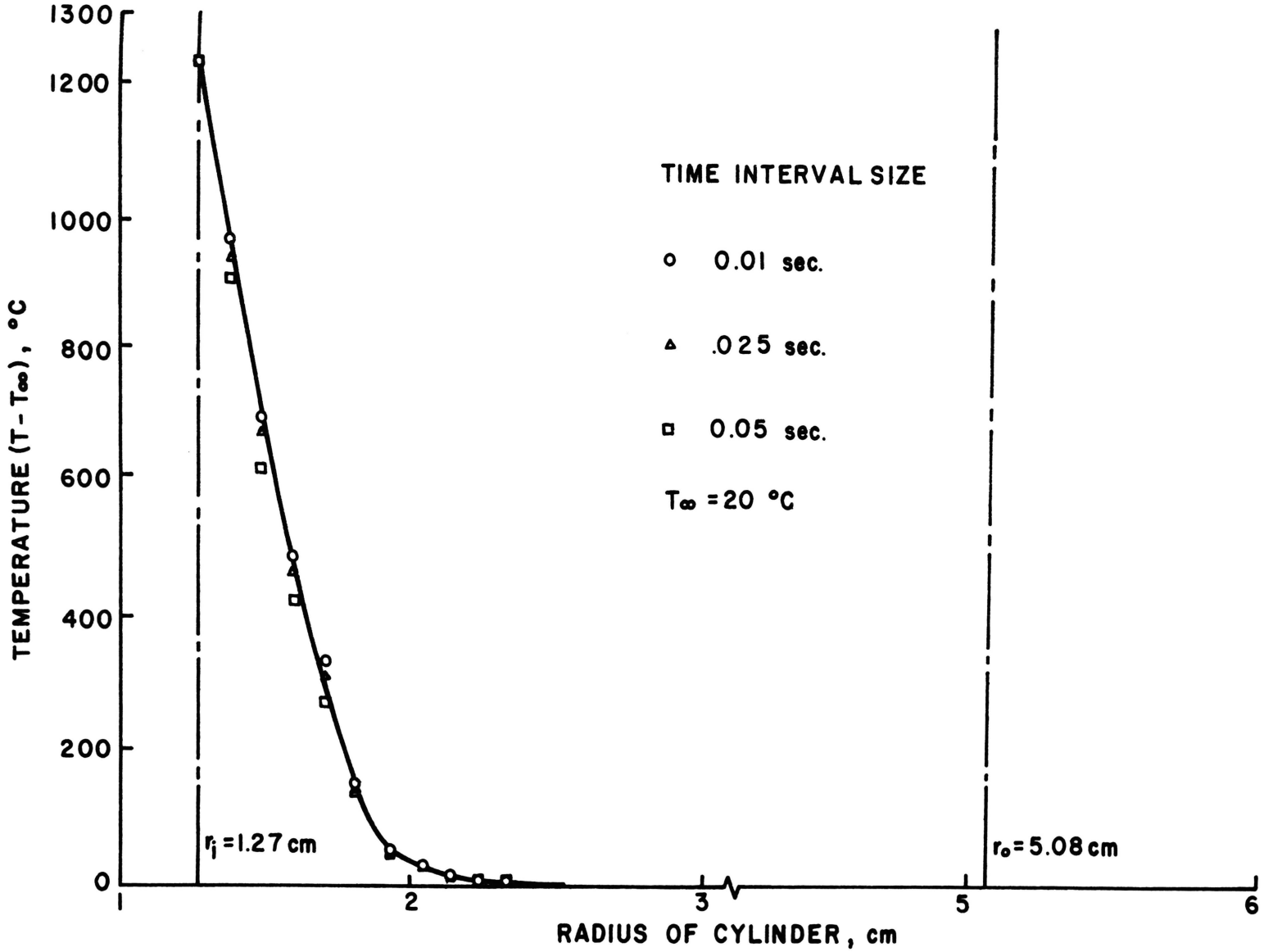

Figure 4 Temperature Distribution across the Cylinder after .05 Seconds

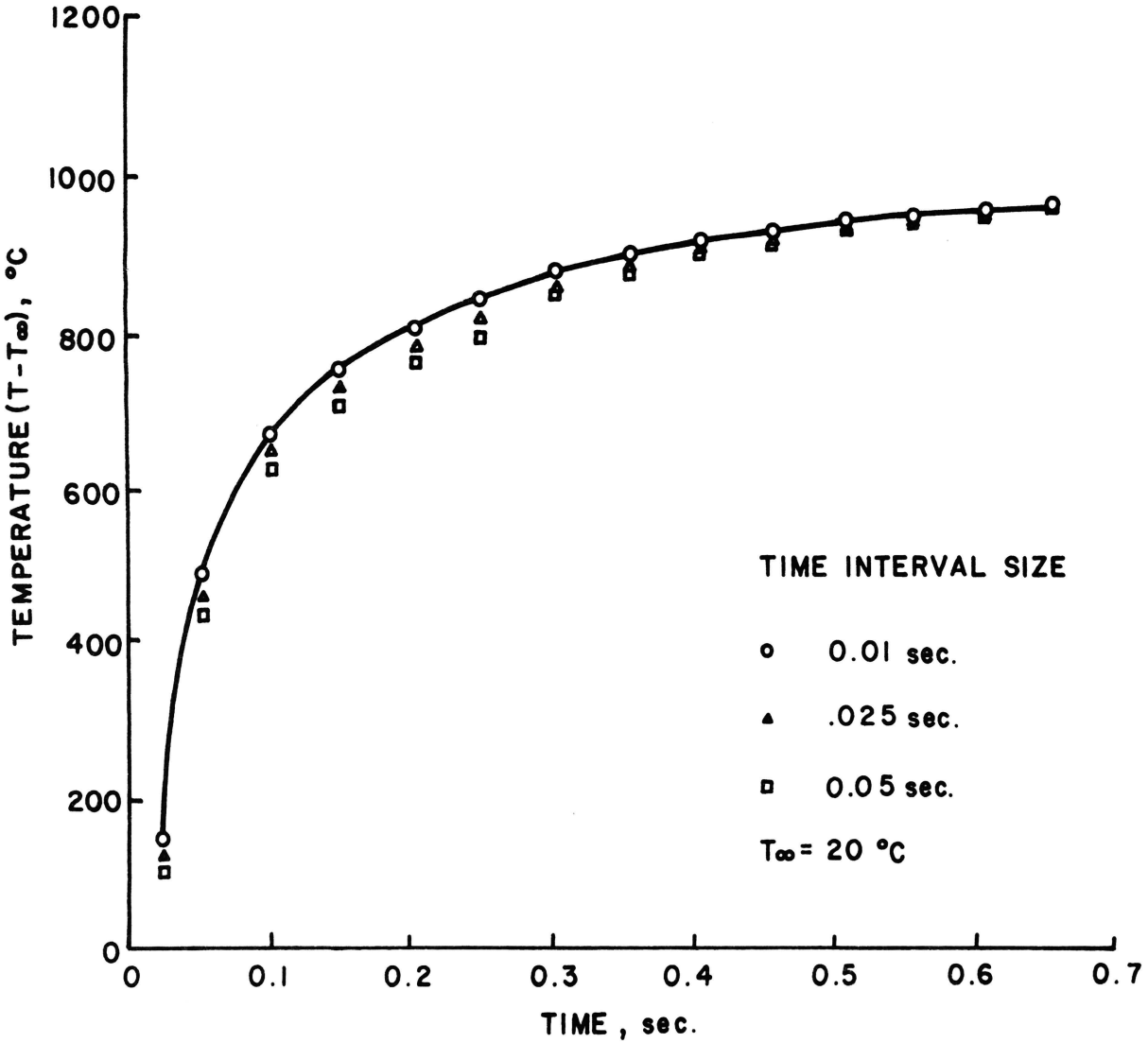

Figure 5 Temperature History at 1 mm. from the Heated Surface

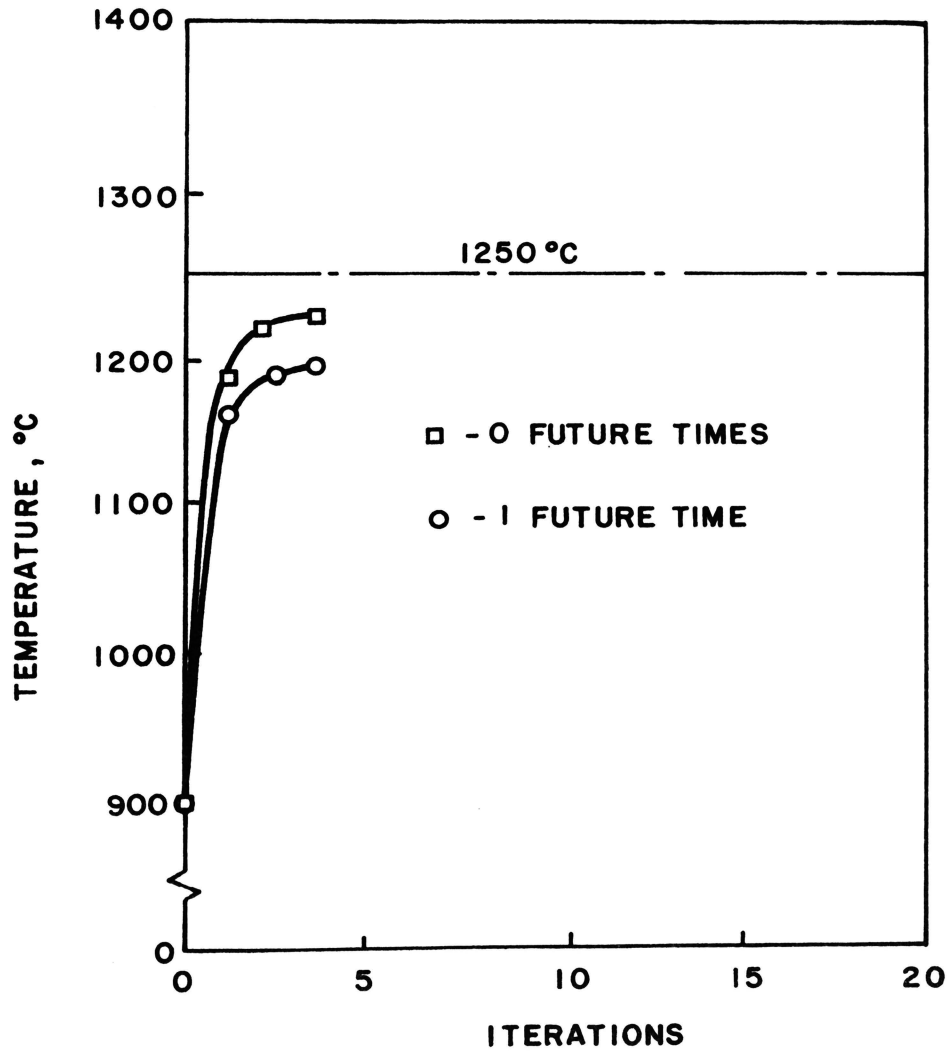

Figure 6 Surface Temperature from Inverse Solution

perature in calculating the average element temperature.

The size of the surface temperature change is not known when solving an inverse problem and must be estimated. When the material properties are temperature dependent, the initial estimate of the boundary condition must be near the exact value. In this example the initial estimate of the surface temperature was 900°C and the correct surface temperature was 1250°C. The large difference in estimated initial temperature and final temperature indicates that the initial estimate was considerably in error. A closer estimate of the exact surface temperature could be made and the inverse resolved to obtain a more accurate solution. The initial estimate was changed to 1230°C. The final result of the iteration was to within .5% of 1250°C.

It should be noted that the initial estimate must be changed only for a step change in surface temperature for materials with temperature dependent material properties. Since a step change in surface temperature cannot occur in a physical problem, this difficulty will not be encountered with experimental data.

Example 2

The boundary conditions for the direct problem of this example are

$$T(r_i,t) = f(t) \qquad t > 0 \qquad (3.39)$$

$$T(r_0,t) = 20.0 \qquad (3.40)$$

$$T(r,t) = 20.0 \qquad t \leq 0 \tag{3.41}$$

The material properties for both the direct and inverse problems were

$$K(T) = .1T \tag{3.42}$$

$$C(T) = .1T \tag{3.43}$$

$$\rho = 1.0 \tag{3.44}$$

In this example the direct finite element program was used to generate the internal temperature resulting from an imposed surface temperature. The properties for this example were also adjusted to allow a small temperature change to produce a noticeable change in material properties. In addition four internal temperature histories corresponding to four internal points were used rather than one. This corresponds to experimentally measuring the temperature at four different depths. The data for each of the four points was equally weighted. The results of the inverse are shown in Figure 7.

E. Inverse Finite Element Program

The basis for the inverse method is the program 2DNLT. Nonproprietary details of 2DNLT are given in Chapter II. The inverse program was called "INVRS". A flow chart for modifying 2DNLT so that it could be used as an inverse program is given in Figure 8. The INVRS program is available within the RMERC for future research, thus, the input data instructions are included in Appendix C.

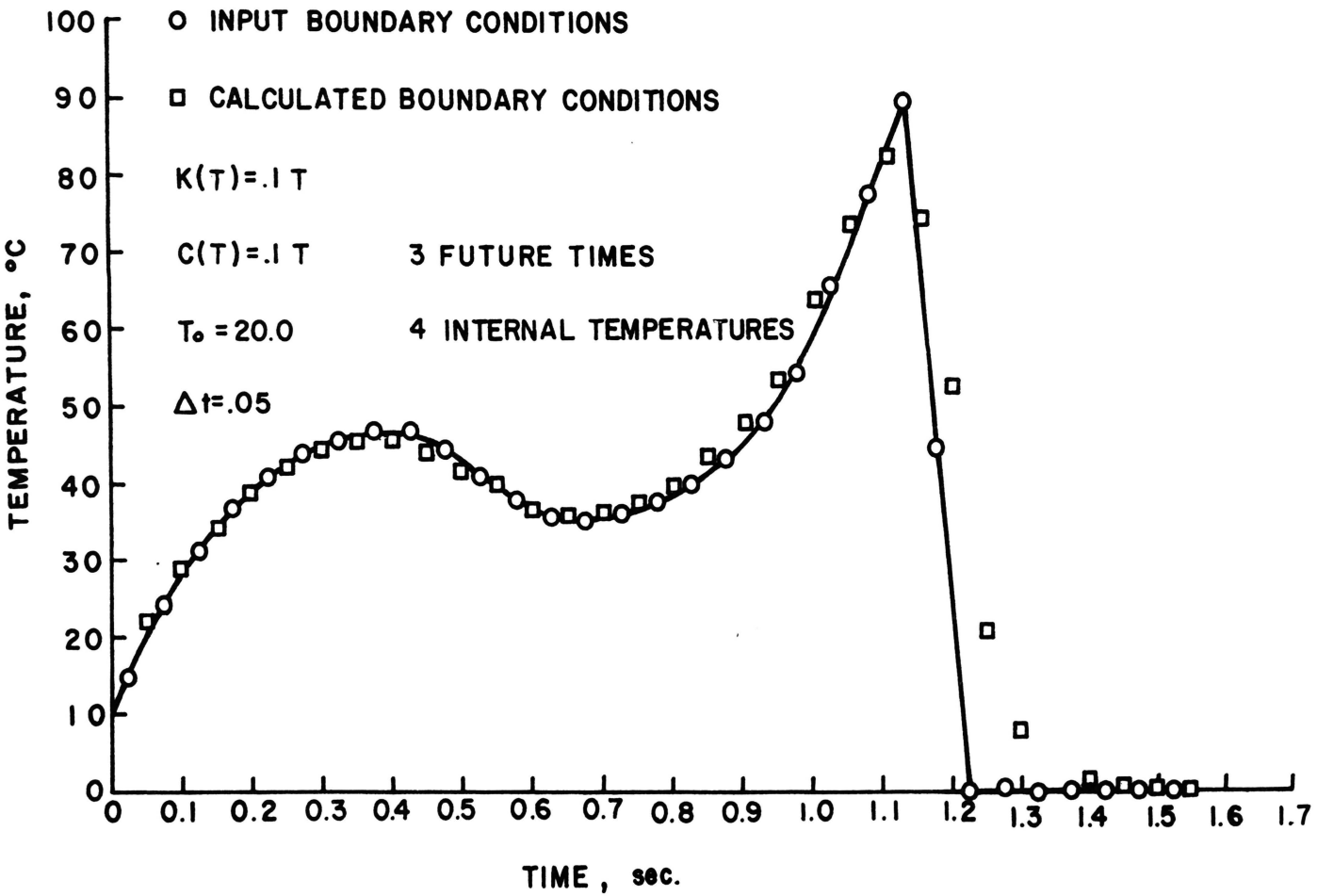

Figure 7 Surface Function for the Inverse Test Problem

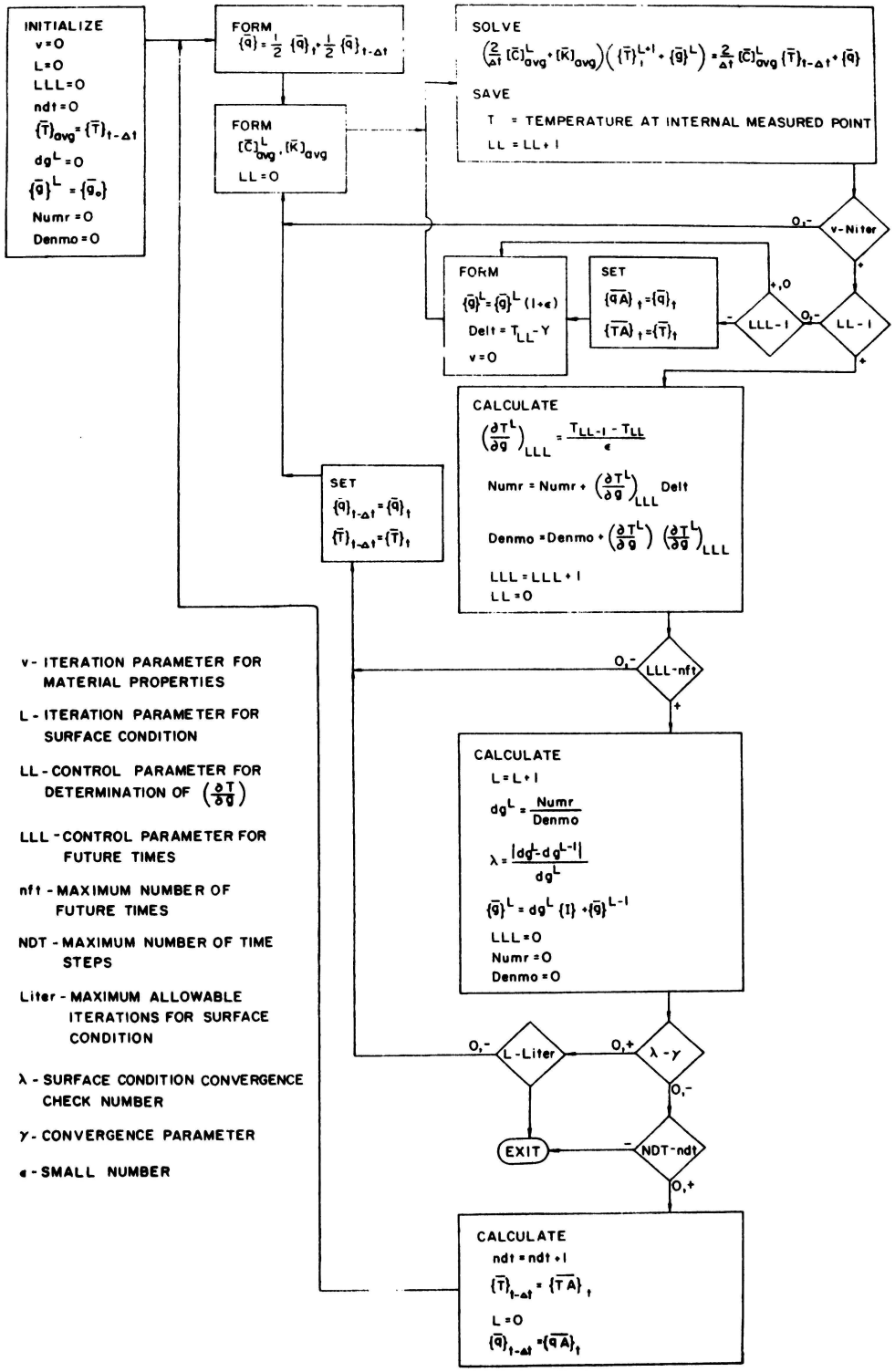

Figure 8 Flow Chart (INVRS)

IV. FUTURE TIME CONSIDERATIONS BASED ON WAVE SPEEDS

When smaller and smaller time intervals are used in the numerical solution of an inverse problem, the procedure may become unstable. A procedure to increase the stability of the numerical method is to use more than one time interval in the inverse analysis. Beck (31) has shown that the additional time intervals aid stability by allowing the internal points more time to respond to a surface change. However, using more than one time interval in an inverse solution reverses the process of decreasing the time interval size. The full benefit of reducing the time interval size is not obtained when additional time intervals are used. However, reducing the time interval size can allow a more accurate direct solution thereby improving the inverse solution. Beck (31) called the additional time intervals, future times. The question of how many future times should be taken can be found by trial and error or the procedure outlined by Beck. He does not give the number of future times for all types of inverse problems. The procedure must be applied for each new inverse problem.

An alternate procedure is to consider a surface temperature change and estimate the delay time for an internal point to respond to the surface change. Additional time intervals would allow the internal points time to respond

to a surface change.

The existance of thermal waves and the possibility of establishing them in material has been employed to find thermal properties (55). If the speed of propagation of a thermal disturbance is known, then the time for the thermal disturbance to travel from one point to another can be calculated. The time for a surface thermal disturbance to propagate to an internal point is the delay time. The solutions that are available for analysis of thermal waves are made up of a transient term and a quasi-steady state term. The transient term quickly dies out and all that is left is the quasi-steady state term. A sinusoidal surface temperature variation of a half space has a quasi-steady state term called a plane progressive damped temperature wave. The wave speed for a plane progressive damped wave has been calculated (17).

$$\nu = \sqrt{\left(\frac{2K}{\rho C}\ \omega\right)} \qquad (4.1)$$

where

ν = wave velocity

ω = frequency of the thermal wave

K = thermal conductivity

ρ = density

C = heat capacity

A. Calculation of Delay Time

Since classical heat conduction is to be used as a basis for solution of the inverse heat conduction problem, then classical heat conduction should be used for finding delay time. Some assumptions will be made to facilitate approximating the delay time.

1. Constant Material Properties For a small time step this assumption should not introduce serious errors.

2. Half Space For times near zero and points near the surface, this geometry should also approximate a sphere or cylinder.

3. Plane Progressive Damped Temperature Wave The velocity for this type of wave is already available (17).

With these conditions in mind one can directly proceed to find the delay time, T, which is a function of depth, frequency and material properties and can be found from the wave velocity, ν, and the depth, d, of the internal point.

$$T = \frac{d}{\nu} \tag{4.2}$$

where

d = distance from the surface to an internal point

T = time for thermal wave to travel from the surface to an internal point, or delay time between a surface change and the internal response

then

$$T = d\sqrt{\frac{\rho C}{2K\ \omega}} \tag{4.3}$$

Thus, for a given frequency and constant material properties, the delay time is directly proportional to the depth. To determine a relationship between a surface change and the time delay before the effect of the surface change reaches an internal point, consider the first quarter of a cycle as shown in Figure 9.

Let the first quarter of the sine curve represent a change in the surface conditions that occurs over one time interval. The smaller time interval sizes, the more accurate this approximation becomes. Expressing the time interval size in terms of the frequency of the sine curve in Figure 9

$$\Delta\tau_0 = \frac{\tau}{4} = \frac{1}{4}\left(\frac{2\pi}{\omega}\right) \tag{4.4}$$

where

$$\begin{aligned} \Delta\tau_0 &= \text{time interval size} \\ \tau &= \text{period of surface change} \\ \omega &= \frac{\pi}{2\,\Delta\tau_0} \\ &= \text{frequency of surface change} \end{aligned} \tag{4.5}$$

The delay time in terms of time steps is

$$T = d\sqrt{\frac{\rho C}{K\pi}\,\Delta\tau_0} \tag{4.6}$$

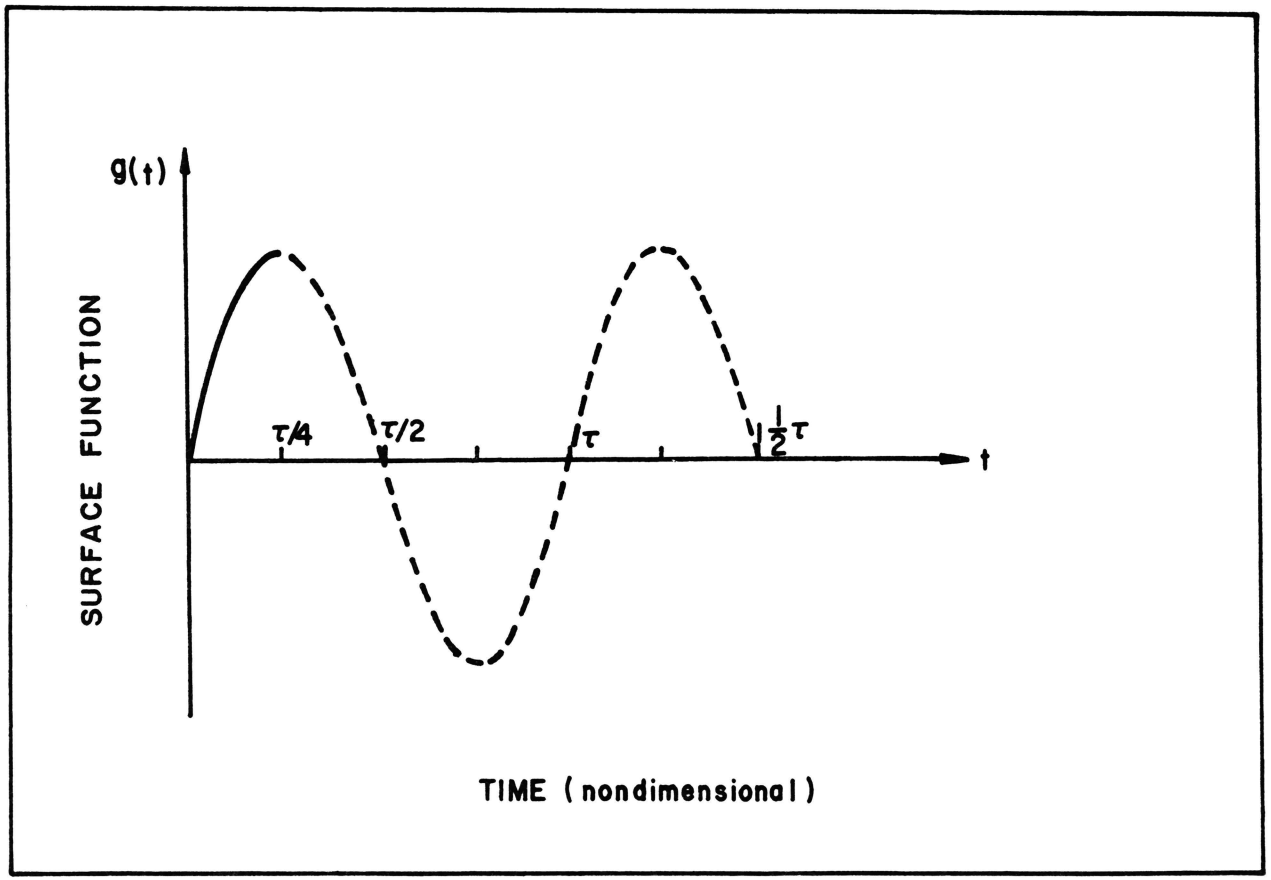

Figure 9 Assumed Surface Function

If the delay time is expressed as a function of the time step size, then

$$T = N \Delta \tau_0 \tag{4.7}$$

and substitution into Equation (4.6) gives

$$N \Delta \tau_0 = d \sqrt{\frac{\rho C}{K \pi} \Delta \tau_0} \tag{4.8}$$

or

$$N = d \sqrt{\frac{\rho C}{K \pi \Delta \tau_0}} \tag{4.9}$$

and

$$N^2 = (d^2 \frac{\rho C}{K}) \frac{1}{\pi \Delta \tau_0} \tag{4.10}$$

Let

$$\Delta \tau = \frac{\Delta \tau_0 K}{d^2 \rho C} \tag{4.11}$$

then

$$N^2 = \frac{1}{\pi \Delta \tau} \tag{4.12}$$

If a time step size is selected, then the corresponding number of time steps required for the change to be felt at the internal point is given approximately by Equation (4.12).

The assumption of Equation (4.4) requires that the period of surface variation cannot be any shorter than four times the time step. In terms of frequency

$$\omega_{surface} \leq \frac{\pi}{2 \Delta \tau_0} \tag{4.13}$$

If the frequency content of the surface function is known, an approximate upper limit on the time step can be established as

$$\Delta \tau_0 \leq \frac{\pi}{2\omega_{surface}} \tag{4.14}$$

where

$\omega_{surface}$ = the highest frequency component of the surface function

B. Future Times for Use with Numerical Solutions

Equation (4.12) gives the approximate number of time steps required to tune the internal response to a change corresponding to a sinusoidal input. The total number of time steps of Equation (4.12) is equal to the number of future times plus one

$$N = nf + 1 \tag{4.15}$$

where

nf = number of future time steps

Substituting for n in Equation (4.12) gives

$$(nf + 1)^2 = \frac{1}{\pi \Delta \tau} \tag{4.16}$$

Figure 10 shows the following:

1. A plot of Equation (4.16).
2. The point at which instabilities were encountered

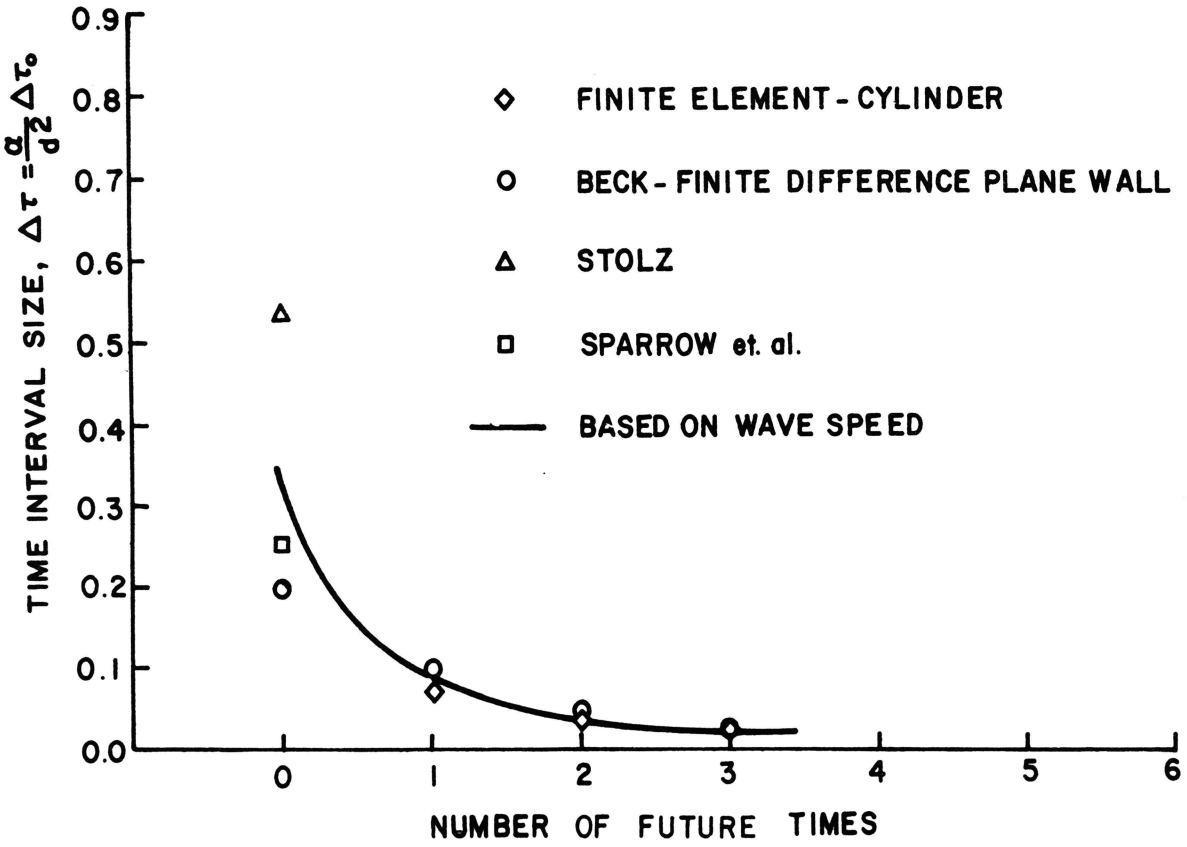

Figure 10 Future Times Versus Time Step Size

by Stolz (18).

3. The point at which Sparrow (25) predicted temperatures in advance of the current time step would be needed.

4. Beck's (31) recommended points for a plane with one insulated surface.

5. Points obtained from a finite element program using Beck's procedure for a hollow cylinder with convection on the outer surface.

V. EXPERIMENTAL DATA

A series of experimental tests were run to obtain temperature data for use with the inverse method and provide fracture data for a preliminary fracture study. The experimental tests were designed to be similar to large scale thermal fragmentation tests being conducted by the Rock Mechanics and Explosive Research Center, University of Missouri-Rolla (46). The Rock Mechanics and Explosive Research Center will be abbreviated as RMERC throughout this dissertation.

A. Discussion of the Experimental Example

A complete discussion of the design of the experimental problem can be found in Chapter IX, reference (46). The heaters were constructed from Kanthal wire coils wound on Alumina cylinders. The test specimens were hollow Dresser Basalt cylinders of four inch outside diameter, one inch inside diameter and the cylinder lengths ranging from nearly one half inch to over eight inches. Figure 11 shows the Dresser Basalt model, heater, thermocouples and end plugs. The Kanthal heater is shown in Figure 12. The entire experimental set up is shown in Figure 13. Figure 14 shows twenty-one of the Dresser Basalt cylinders after they were tested.

1. Modes of Heat Transfer The Kanthal wire of the heater of Figure 12 reaches a temperature of approximately

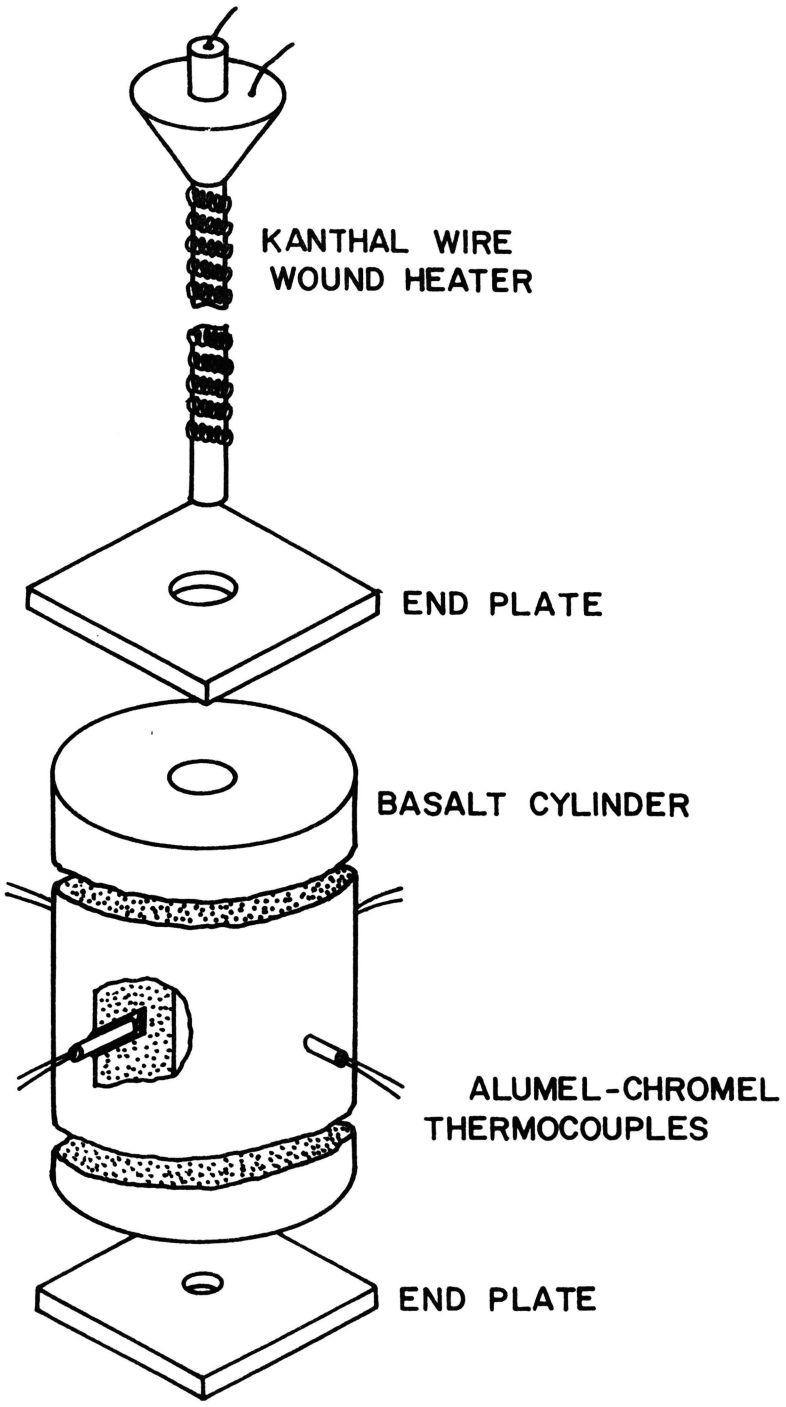

Figure 11 Experimental Model Setup

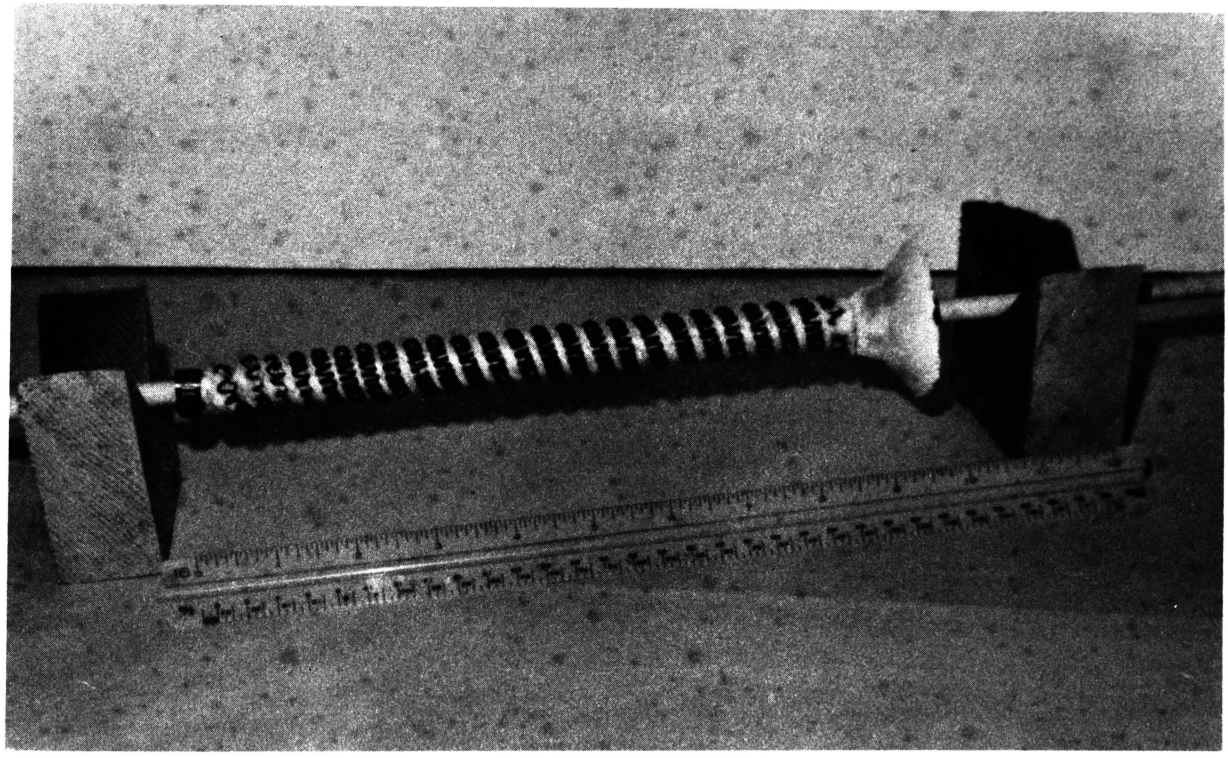

Figure 12 Kanthal Wire Heater

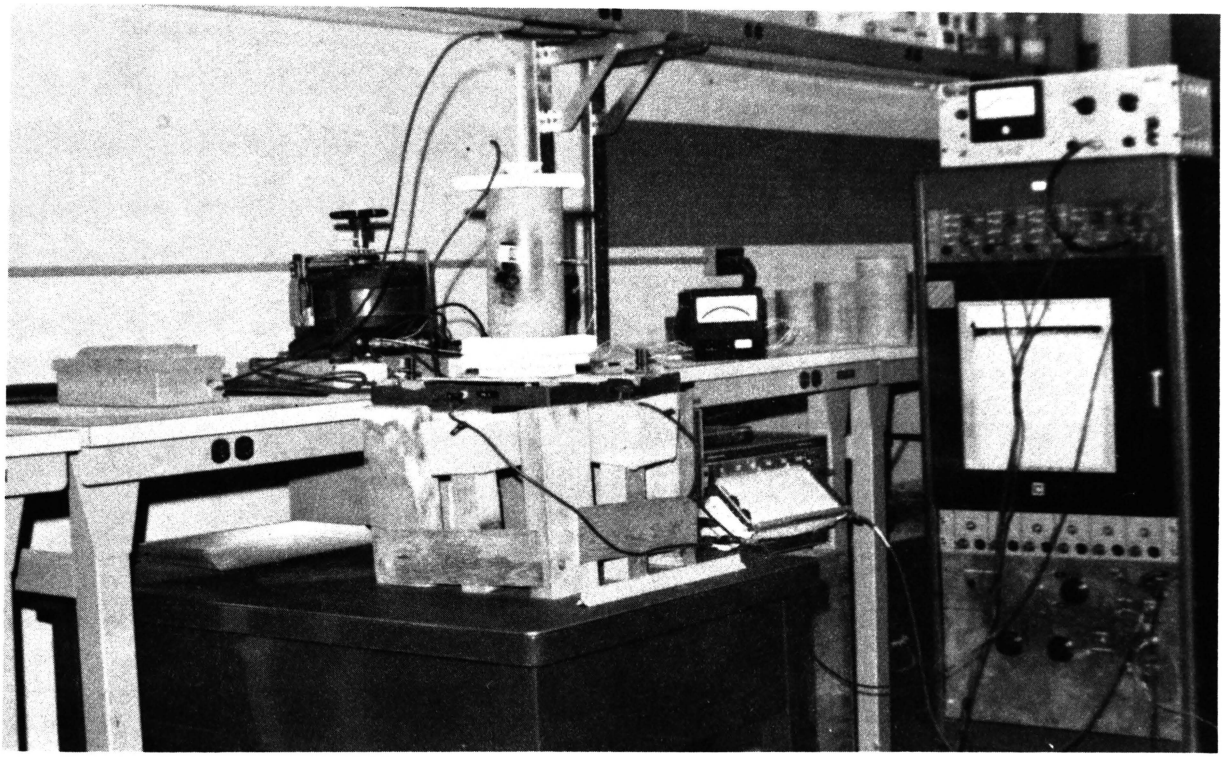

Figure 13 Complete Experimental Setup

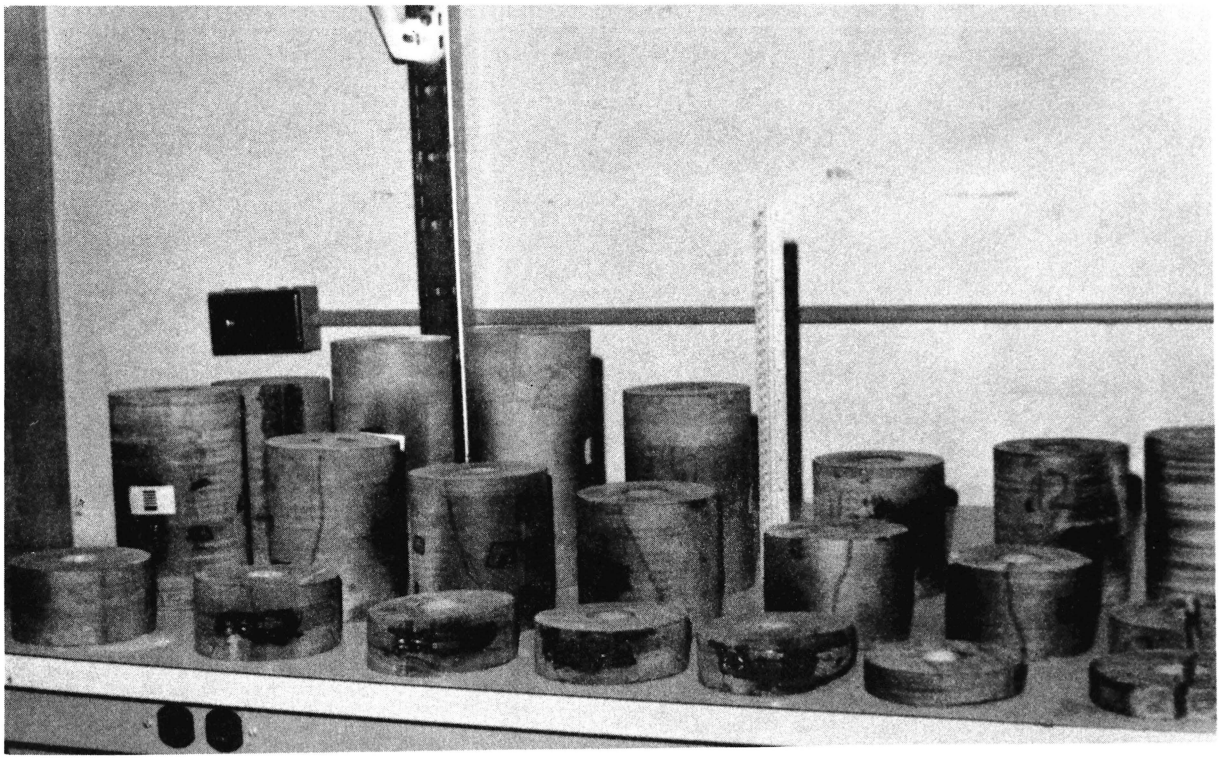

Figure 14 Dresser Basalt Experimental Cylinders

1000°C. The modes of heat transfer from the heater to the rock cylinder are radiation, convection and conduction. The end plates and the tapered section on the heater were devised to partially seal the cylinder and reduce the amount of air entering and escaping the cylinder. This simulated the conditions in the large scale tests where fiber glass was packed at the heater ends to reduce convective currents (46).

Although the convective currents were reduced, there still were noticeable convective currents in both the large scale tests and the experiments of this dissertation. The convective currents were hotter at the top of the cylinder than at the bottom because cool air entered at the bottom and was heated as it rose past the heater and exited at the top of the cylinder. The top of the cylinder was consequently hotter than the bottom of the cylinder. The temperature difference between the two ends of a cylinder was greater as the length of the cylinder was increased.

2. Design of Heat Transfer Test Specimens The effect of the convective currents was neglected in the design of the test specimens. The experimental cylinders were designed so that conduction through the end plates would have a small effect on the center plane temperature. The lengths of the four cylinders used for the temperature measurements were chosen so that the internal heat

transfer would be nearly one dimensional for a steady state problem with a constant temperature applied to the inside surface. The lengths of the cylinders that were used to obtain the experimental temperature data were all greater than seven inches. Thus, the heat flow at the middle of the cylinder and the surface temperature at the middle of the cylinder would not be appreciably influenced by conduction through the ends of the cylinder (46).

3. Fabrication of Test Specimens The hardness of Dresser Basalt requires special machining to produce experimental specimens. Diamond impregnated core drills were used to make the four inch diameter cylinders from large pieces of Dresser Basalt. The Dresser Basalt cylinders were then mounted on a lathe and a one inch diameter core removed with a diamond core drill. The cylinders were cut to the desired lengths with a diamond saw. The large size of the test specimens and the great hardness of the Dresser Basalt prevent any of the machining procedures from being performed with extreme accuracy. The most precise procedure was the location of the center hole. The holes for the thermocouples were made with a high speed diamond drill. The location of the holes for the thermocouple probes was as accurate as possible using good machine shop practices.

4. Specimen Instrumentation Twenty-one Dresser Basalt cylinders had a platinum resistance temperature

gage and a strain gage mounted on the outside surface at the center plane and 180° apart. The strain gages gave an indication of the tangential strain and also a clear indication of when fracture occurred. Four of the twenty-one specimens had four 1 mm. holes drilled radially in them at their center plane and 90° apart. These holes were used for alumel-chromel thermocouples. The thermocouples were located at 1 mm., 2 mm., 3 mm., and 4 mm. from the inside surface. To insure the best possible contact between the thermocouple and the Dresser Basalt, the thermocouple assembly was spring loaded.

Four additional Dresser Basalt cylinders were prepared and tested without any gages or thermocouples attached. These four cylinders were used as a supplemental test to study the effect of the convective currents. All four cylinders of the supplemental test were approximately one half inch in length.

Wiring diagrams and a list of equipment can be found in Appendix D.

5. Experimental Procedure The heater was placed inside the Dresser Basalt cylinder and the electrical power to the heater was quickly increased from zero to full power. This heating procedure is similar to the procedure employed in the large scale tests (46). The recording of internal temperatures, outer surface temperature and tangential strain began with the application of

power to the heater. When short cylinders were tested, they were placed against the bottom end plate and the top end plate was placed on top of the specimen. For short cylinders the heater extended through the top end plate into the open air.

After the initial fracture data was obtained for twenty-one cylinders, another series of fracture tests were performed on four additional cylinders. All of these cylinders were approximately one half inch in length. Two of the four cylinders were tested in the same manner as all of the previous cylinders. The other two were tested with a five inch Dresser Basalt cylinder placed beneath them to simulate the heat transfer conditions of a five and one half inch cylinder. These four cylinders did not have strain gages so the noise of fracture was used to indicate fracture. The time to fracture was measured with a stopwatch.

B. Experimental Temperature Data

The curves of Figure 15 are a representative example of the data obtained from the four cylinders that had thermocouples. Over the temperature range encountered by the thermocouples, the diffusivity has only a small change. If the heat transfer was one dimensional and the Dresser Basalt homogeneous, then the curves of Figure 15 should show a pattern of internal temperature histories

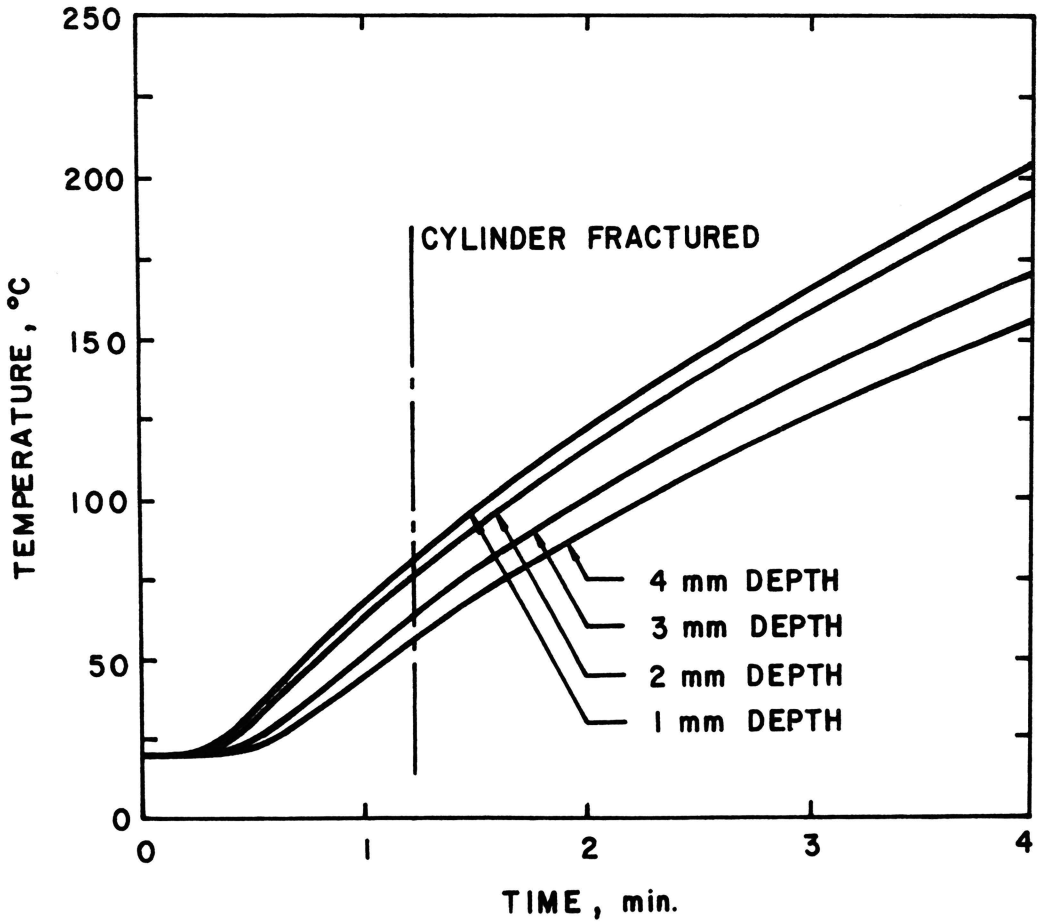

Figure 15 Temperature Variation with Time for a Typical Dresser Basalt Temperature Test

similar to that of a linear material. This is, however, not the case as can be seen by the fact that the temperature difference between the curves going from the 1 mm. to the 4 mm. curve shows no linear pattern. This may be caused by the inhomogeneity of the Dresser Basalt or by the design of the Kanthal heaters. In Figure 11 it is evident that one thermocouple may be directly opposite a heater coil, while another may be opposite a space between the coils. This influence will, of course, be diminished as the distance from the inside surface to the thermocouple is increased. The contact area between the top of the spring loaded thermocouples and the Dresser Basalt would be difficult to accurately predict. Each thermocouple had a slightly different contact area.

C. Experimental Fracture Data

The strain gages on the rock cylinders provide tangential strain measurements as a function of time for the Dresser Basalt cylinders. The time to fracture was marked by a sharp drop in tangential strain. This sharp drop in tangential strain was accompanied by an audible noise. Based on the sharp drop in strain and the noise of fracture, it was assumed that a crack initiated and then rapidly propagated. Figure 16 shows the time to fracture for different lengths of test cylinders.

A total of twenty-one cylinders were used in the

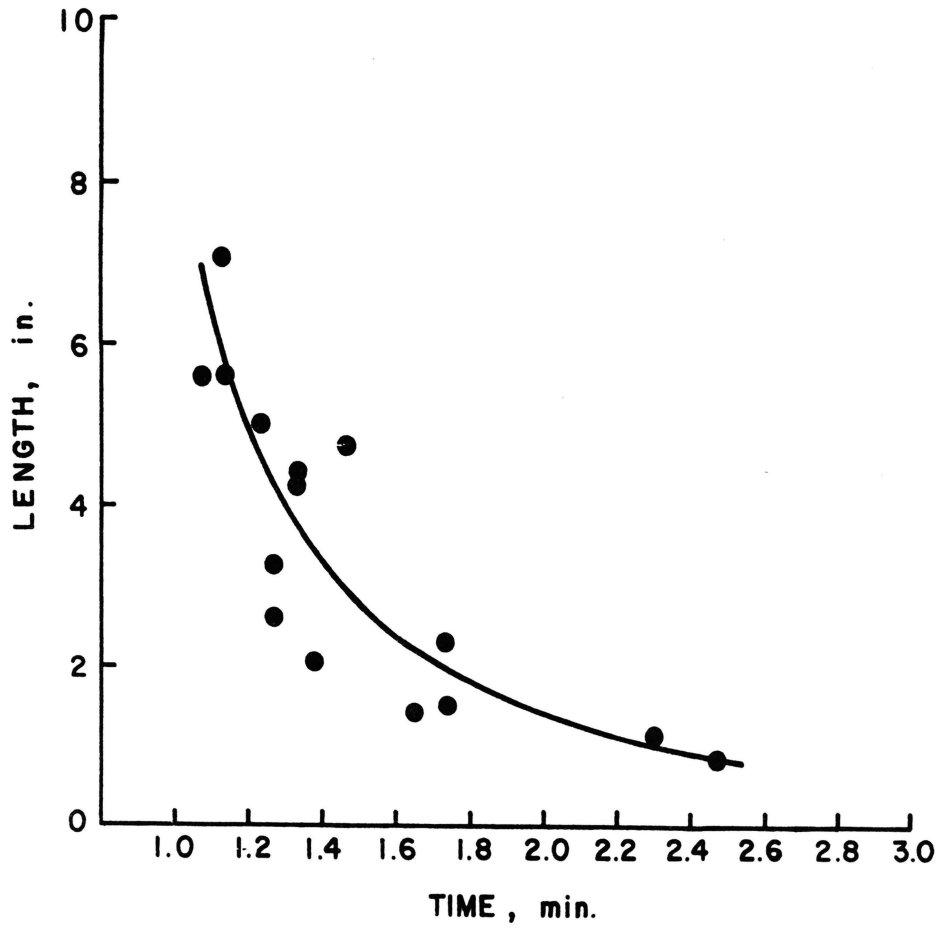

Figure 16 Time to Fracture for a Dresser Basalt Cylinder

initial experimental study. Fracture data was obtained on fifteen of the twenty-one cylinders. Two cylinders were used for preliminary studies and four cylinders had pre-existing cracks.

D. Supplemental Tests

The supplemental tests were designed to indicate if the heat transfer conditions at the top of the cylinder controlled the time to fracture. Four cylinders of approximately one half inch in length were tested. Two of the cylinders were tested in the same manner as the previous twenty-one cylinders. These two cylinders encountered heat transfer conditions similar to the bottom of a long cylinder. The other two cylinders were placed on top of a five inch Dresser Basalt cylinder and then tested. Thus, the second two cylinders encountered the same heat transfer conditions as the top one half inch of a cylinder which is five and one half inches long.

Figure 17 shows the fracture trend line from Figure 16 and the additional four data points. The controlling factor for time to fracture can be seen in Figure 17 to be the heat transfer conditions at the top of the cylinder.

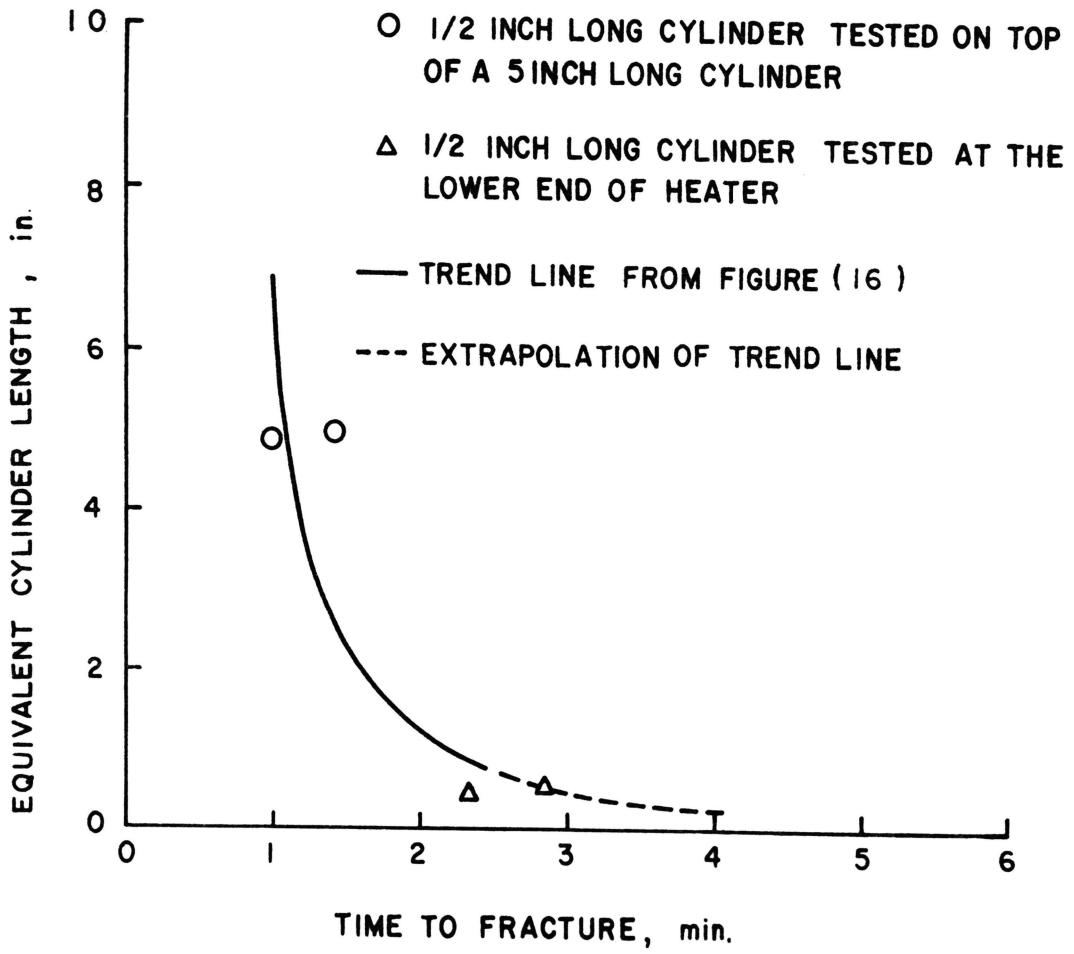

Figure 17 Supplemental Fracture Data

VI. APPLICATION OF THE INVERSE METHOD

One use of the inverse method is as part of a thermal stress and fracture study. The inverse method makes use of experimental data to find surface heat transfer conditions. The surface heat transfer conditions are used with the direct method to find temperature distributions for use in a thermal stress analysis.

The experimental heat transfer data of Chapter V was used with the inverse method to find surface temperatures. The surface temperatures were used to find the temperature field, thermal stresses and the resulting time to fracture for a simple model.

Once experimental data is obtained, there are some considerations to be made before proceeding to the inverse solution. These considerations are: boundary condition, boundary condition improvement, finite element models, and future times.

A. Boundary Condition g

The selection of a surface or boundary condition consists of two parts, the first being the assumption of a surface heat flux or surface temperature and the second, the time variation of the boundary condition.

1. Selection of Type of Boundary Condition The selection of a surface heat flux may cause difficulties in the solution of some problems where the conductivity and

heat capacity are very small and the material properties are temperature dependent. A small change in surface heat flux can result in a large change in internal temperature if the conductivity and heat capacity are very small. A large change in internal temperature can produce significant changes in material properties. This creates a problem when numerically evaluating the internal response $(\partial T/\partial g)$ for use in Equation (3.24).

A temperature boundary condition does not have the same difficulty since a small change in surface temperature will also produce a small change in internal temperature. If the material properties are not temperature dependent, the temperature boundary condition assumption quickly looses this advantage over the surface heat flux assumption.

Dresser Basalt was treated as a material with temperature dependent material properties. The conductivity and heat capacity of Dresser Basalt are small. The boundary condition was assumed to be a surface temperature.

2. Selection of a Time Variation of the Boundary Condition The simplest assumption is that the boundary condition is constant for each time step. A constant assumption is a good first assumption for most inverse problems. If the results from the inverse based on a constant assumption indicate a linear variation of the boundary condition across a time step, then the constant

assumption can be changed to a linear assumption. The inverse program INVRS was programmed for a constant boundary condition for each time step.

B. Boundary Condition Improvement

The simplest assumption for a boundary condition improvement dg is that the improvement is a constant for each time step. A constant improvement allows $(\partial T/\partial g)$ to be easily evaluated numerically, as well as, a simple form of dg for solving Equation (3.24). The program INVRS was programmed for dg to be constant for each time step.

C. Finite Element Models

The accuracy of the inverse solution depends on how well the finite element model describes the experimental model. The accuracy of the inverse solution also depends on the accuracy of the experimental temperature data and the material thermal property data. Thus, a highly sophisticated finite element model for inaccurate experimental data or inaccurate material property data would not be logical. To show the effect of the model on the solution, three different finite element models were used. The effect of an error in material thermal properties on the inverse solution was studied using one of the finite element models.

1. First Model The first model was an axisymmetric hollow cylinder of Dresser Basalt as shown in Figure 18.

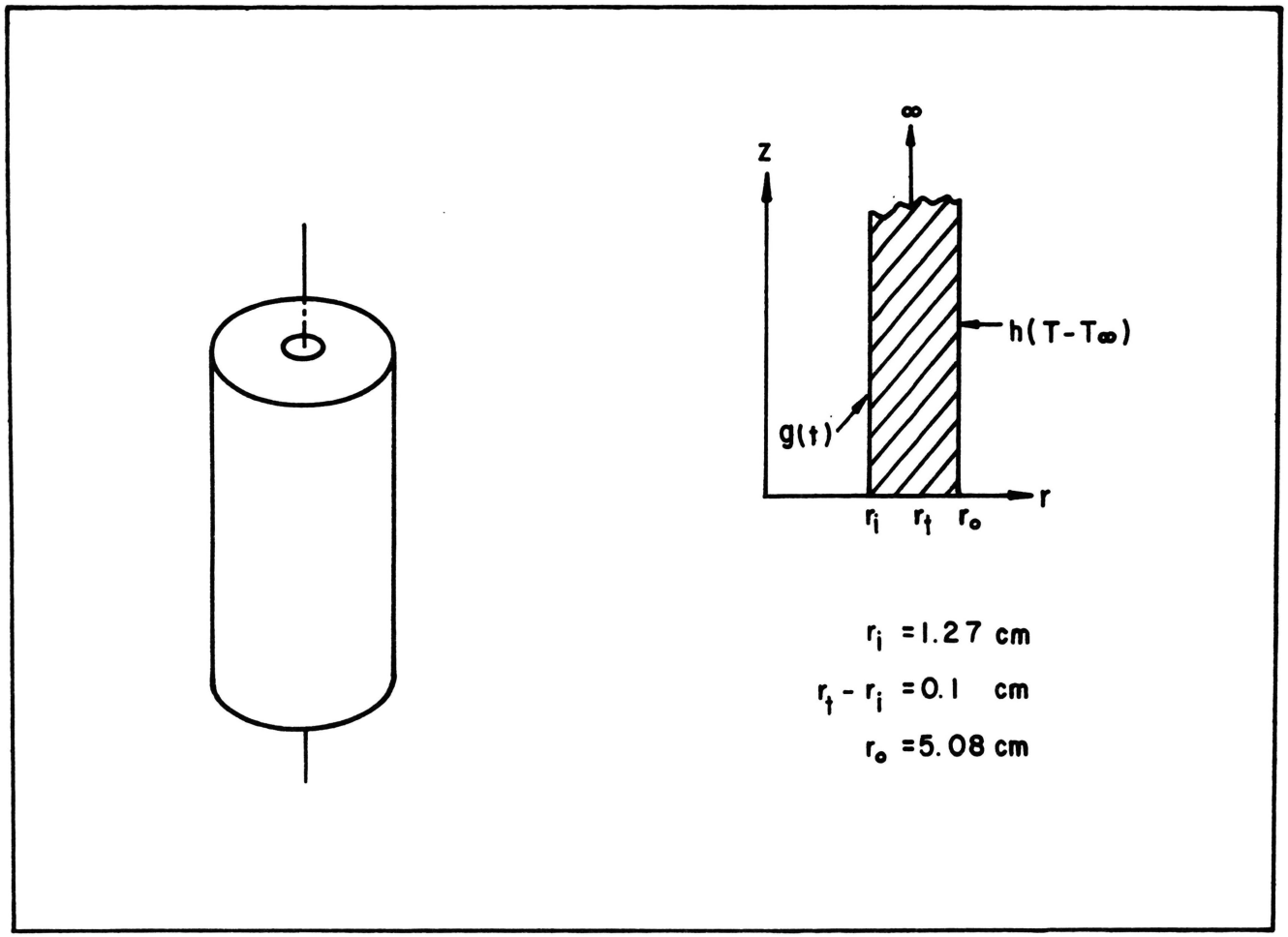

Figure 18 Infinite Cylinder Model

No attempt was made to account for distortion of the temperature field inside the cylinder caused by the thermocouple. No attempt was made to account for the temperature variation along the length of the cylinder due to the coils in the heater or convective currents inside the cylinder. The temperature distribution in the cylinder was assumed to be only a function of time and the radius of the cylinder. The heat flow in this model was one dimensional. The outside boundary condition was assumed to be convection. The finite element model had forty elements. Three equally sized, square elements were between the surface and the 1 mm. point where the internal temperature was measured. Node points were also located at 2 mm., 3 mm. and 4 mm. distances from the inside surface.

2. Second Model The second model was one-eighth of a Dresser Basalt cylinder with an alumel-chromel thermocouple, an omegatite insulator and an air space. This model attempts to account for some of the disturbances of the temperature field caused by the thermocouple. The heat flow in this model was two dimensional. Again, no attempt was made to account for the nonuniformity of the heating of the internal surface. Figure 19 shows the model and Figure 20 shows the finite element grid for the model. There were 226 elements and 248 nodes.

Material properties were needed for air, alumel-

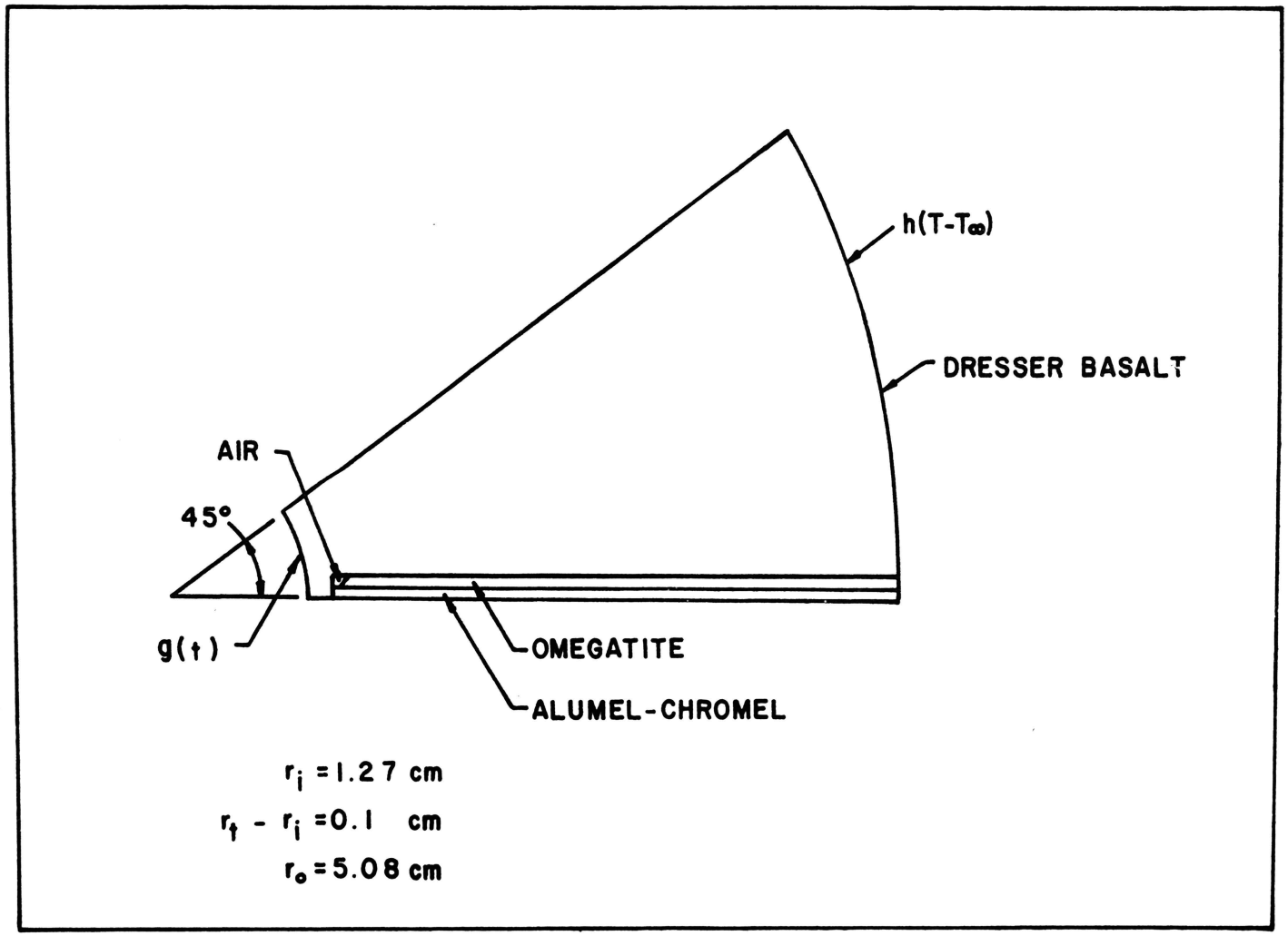

Figure 19 One-eighth of a Cylinder Model--Four Materials

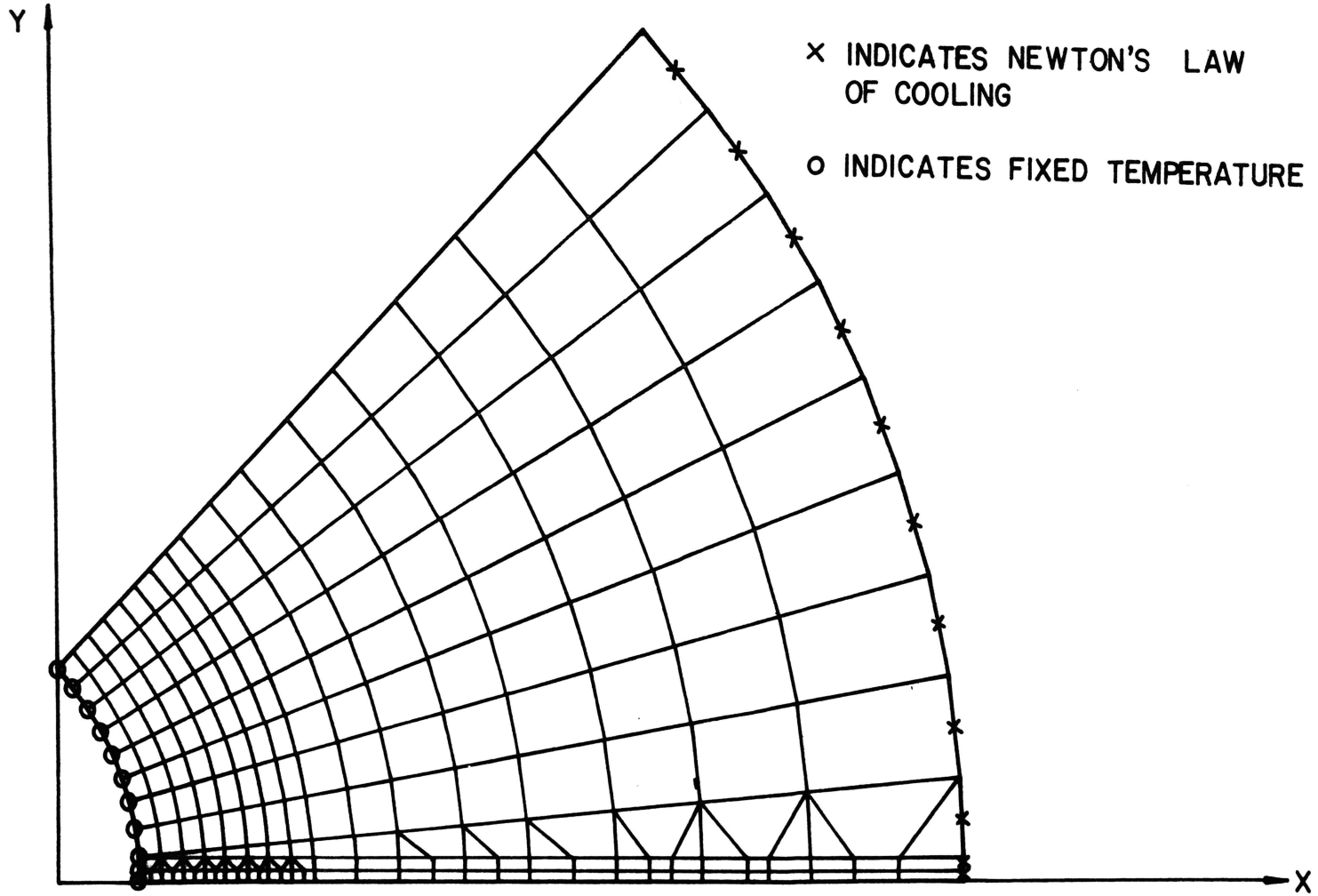

Figure 20 Finite Element Grid for the One-eighth Cylinder Model

chromel and omegatite. The material properties for these materials were assumed to be constants and were approximated from available information (45, 46, 56, 57). The material properties were input in the same form and units that were used for Dresser Basalt. The finite element program made all necessary conversions to provide a consistent set of dimensional units.

TABLE II

Thermocouple Assembly and Air Thermal Properties

Material	(1/conductivity) (hr ft F/Btu)	Heat Capacity $\left(\frac{\text{cal}}{\text{gram } °C}\right)$	Density (gm/cm)
air	7.1	.24	.0081
chromel-alumel	.045	.1	8.9
omegatite	.0689	.2	3.1

3. Third Model A third model was used to obtain a bound on the influence of the thermocouple on the inverse solution. Figure 21 shows the third model. The model had one dimensional heat flow through 1 mm. of Dresser Basalt to an alumel-chromel thermocouple. All of the heat conducted through the Dresser Basalt was conducted through the thermocouple. This model had forty elements. Three Dresser Basalt elements were located between the surface and the point at which the internal temperature

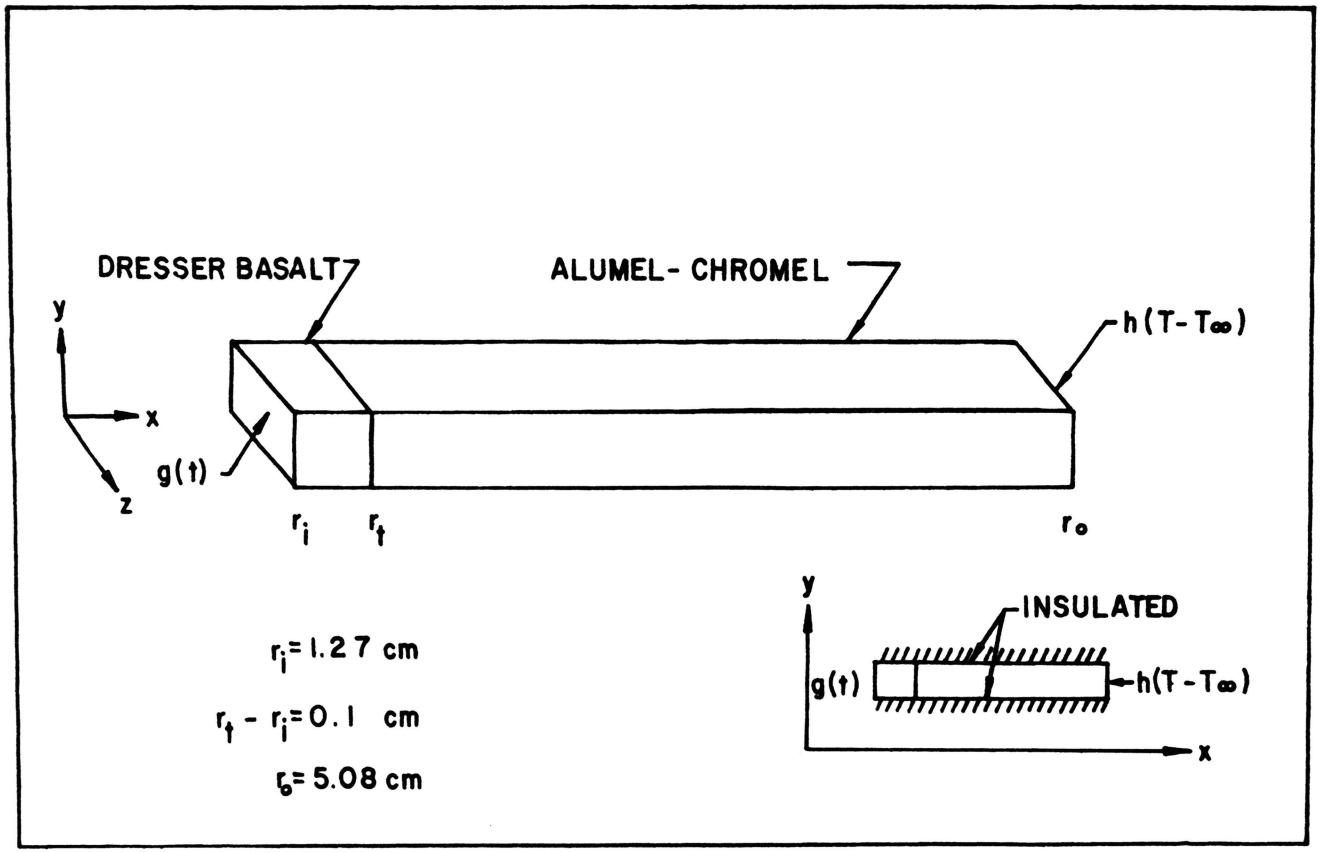

Figure 21 Plane Model--Two Materials

was measured. No attempt was made to account for the nonuniformity of the heating of the internal surface.

D. Future Times

Equation (4.12) was used to determine when future times might be useful. The results for Dresser Basalt and the four thermocouple locations are given in Table III.

TABLE III

Future Times Versus Time Step Size

Number of Future Times	Time Step Size for Each Thermocouple Location 1 mm.	2 mm.	3 mm.	4 mm.
1	1.0	4.0	9.0	16.0
2	.07	.28	.63	1.1
3	.04	.16	.36	.64

E. Results of the Inverse for Experimental Example

Figure 22 shows the results from the inverse program for the three finite element models.

The influence of the thermocouple on the inverse solution can be seen by comparing the results from the first model and the third model. The first model neglects the influence of the thermocouple while the third model insures that the fullest possible influence of the thermocouple is felt. The influence of the thermocouple should be somewhere between the first and the third models. The

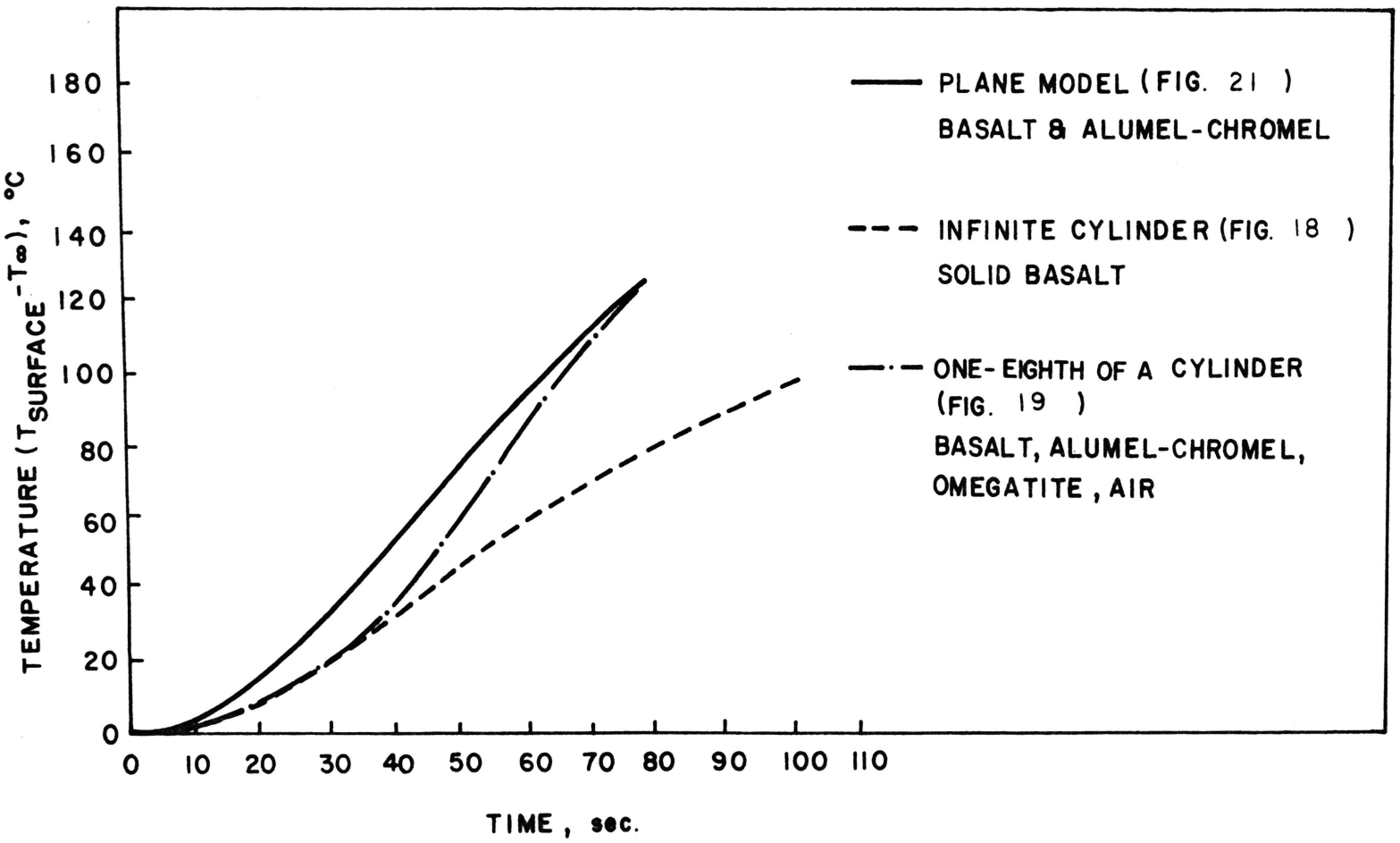

Figure 22 Comparison of Surface Temperature for Different Models and One Internal Temperature

solution of the inverse should, therefore, lie somewhere between the solution for the first model and the solution for the third model. The second model is a better approximation of the experimental model than either the first or the third model. At times less than forty seconds, the influence of the thermocouple on the inverse solution is small, but after forty seconds the influence of the thermocouple becomes much more pronounced.

In general, future times should not be used unless they are necessary to make the numerical procedure stable. If future times are needed, then Table II gives an estimate of the number of future times to use. Time step sizes down to .625 seconds were used and no instability problems were encountered. The inverse solutions were essentially the same for all time step sizes less than 2.5 seconds. Future times were not needed, so they were not used for this example.

The effect of errors in heat capacity and thermal conductivity was checked by assuming them to be in error by ten percent and solving the inverse problem using the first model. The ten percent error in heat capacity had the largest effect but the solution of the inverse did not change by more than two percent.

Model 1 was also used to obtain the inverse solution based on all four thermocouple readings of Figure 15. Figure 23 shows a comparison of the inverse solution for

Model 1 based on the thermocouple at 1 mm. and the inverse solution based on all four thermocouples. As can be seen in Figure 23, the additional thermocouples add little to the final solution.

F. Fracture Prediction Based on the Inverse Solution

The temperature boundary conditions of the three models were used to calculate thermal stresses in a simple model. For both the thermal stress problem and direct heat transfer problems, the finite element models were assumed to be an infinite, hollow, Dresser Basalt cylinder. This model was used to calculate internal temperatures, thermal stresses and time to fracture resulting from the temperature boundary condition on the inside surface of the cylinder.

The outside surface was a convective surface. The inside radius was 1.27 cm. and the outside radius was 5.08 cm. The 2DNLT finite element program was used to solve for the internal temperatures. The finite element grid had forty equal sized elements. Time step size was 2.5 seconds. After the temperatures were calculated, thermal stresses were calculated using the finite element program "TRATSA" (1).

For an infinite, hollow cylinder with heated inside surface and only a radial variation in temperature, the Griffith fracture criteria is satisfied when the tangential

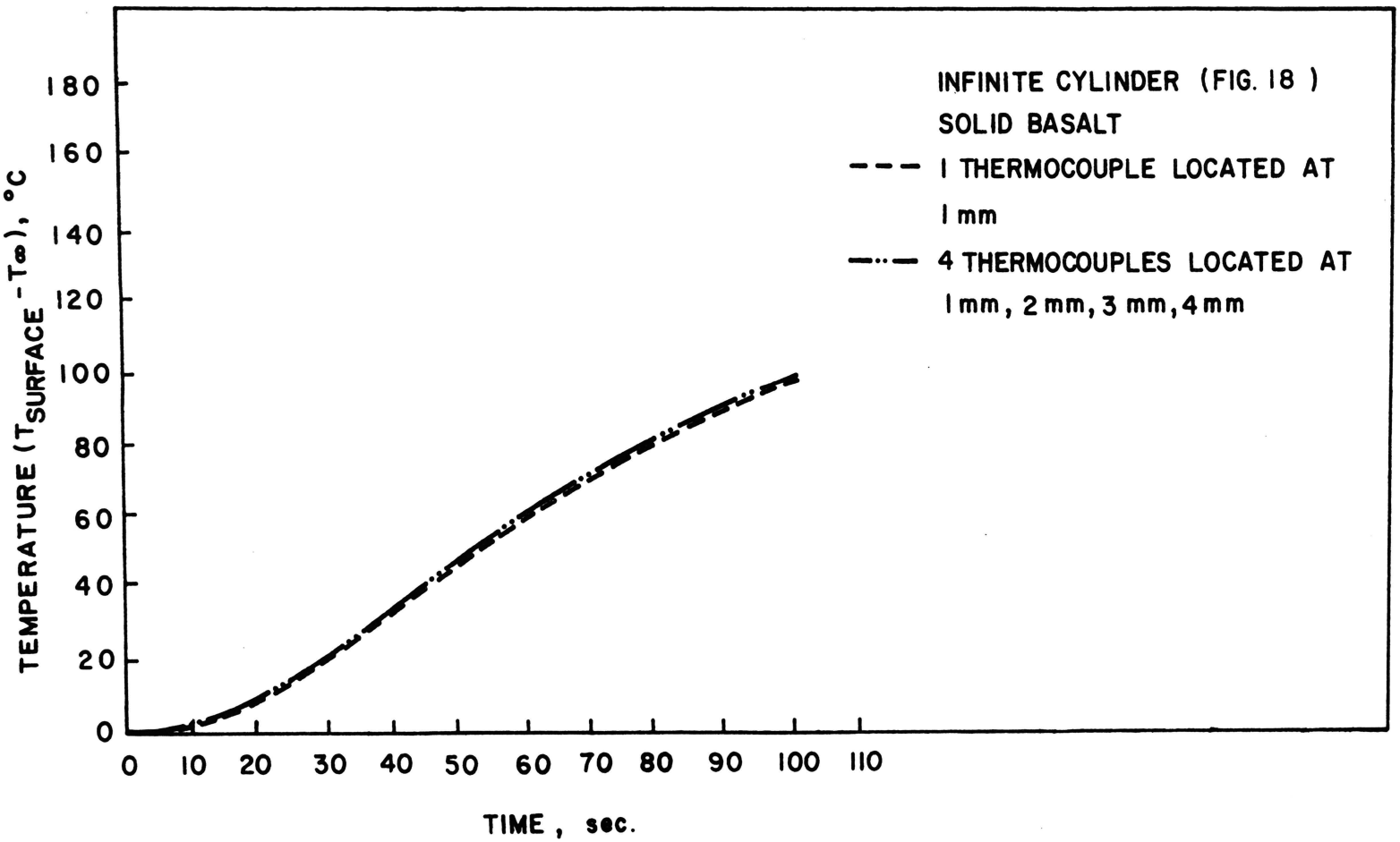

Figure 23 Comparison of Surface Temperature Using One Thermocouple and Four Thermocouples

stress exceeds the tensile fracture stress.

The cylinders were assumed to fracture at the time that the Griffith fracture criterion was first satisfied. The time to fracture for each model is given in Table IV.

TABLE IV

Time to Fracture

Model	Time to Fracture (min.)
First	3.25
Second	2.25
Third	2.0

VII. CONCLUSIONS AND RECOMMENDATIONS

A. Conclusions

Temperature distributions can be approximated in rock material by solving a linearized heat conduction equation. The finite element method can be adapted to linearize the heat conduction equation for temperature dependent materials.

Iteration with a direct heat conduction solution can be used to solve an inverse heat conduction problem. The linearized finite element method can also be used as part of the inverse method.

B. Recommendations

An alternate procedure for solving steady state heat conduction problems was demonstrated which used a thermal load concept. A thermal load concept could be used to include the transient heat conduction problem. An acceleration procedure should be added to the thermal load iteration procedure to speed convergence.

When using the inverse method, future times should not be used unless the results become unstable. If future times are required, Equation (4.12) gives a first approximation of the number of future times to use.

More work must be done to obtain the thermal and mechanical properties of rock materials as a function of temperature. Work must also be done to determine the

dependence of fracture on temperature. Particularly important are the changes in material properties that occur near phase changes.

BIBLIOGRAPHY

1. Patel, M.R., "Rock Fragmentation by Subsurface Thermal Inclusions--A Finite Element Study," Ph.D. Dissertation, University of Missouri-Rolla, 1973.

2. Luikov, A.V., "Methods of Solving the Nonlinear Equations of Unsteady-State Heat Conduction," Heat Transfer--Soviet Research, Vol. 3, No. 3, 1971, pp. 1-51.

3. Emery, A.F. and W.W. Carson, "An Evaluation of the Use of the Finite-Element Method in the Computation of Temperature," Journal of Heat Transfer, Trans. ASME, Series C, Vol. 93, 1971, pp. 136-145.

4. Zienkiewicz, O.C., The Finite Element Method in Engineering Science, McGraw-Hill, London, 1971.

5. Myers, G.E., Analytical Methods in Conduction Heat Transfer, McGraw-Hill Book Company, New York, 1971.

6. Meisner, J., "On the Linear Theory of Heat Conduction," Archive for Rational Mechanics Analysis, Vol. 39, 1970, pp. 108-130.

7. Maxwell, J.C., "On the Dynamical Theory of Gases," Philosophical Transactions Royal Society of London, Vol. 157, 1967, pp. 49-88.

8. Cattaneo, C., "Sulla Conduzione del Calore," Atti del Seminario Matematico e Fizico della Universita di Modena, Vol. 3, 1948, pp. 83-101.

9. Vernotte, P., "La Veritable Equation de la Chaleur," Comptes Rendus Hebdomadaires des Seances, Academie des Sciences, Paris, Vol. 246, pp. 3154-3155.

10. Nettleton, R.E., "Relaxation of Thermal Conduction in Liquids," Physics Fluids, Vol. 3, 1960, pp. 216-225.

11. Chester, M., "Second Sound in Solids," Physical Review Letters, Vol. 131, 1963, pp. 2013-2016.

12. Lykov, A.V., "Primenenie Metodov Termodinamiki Neobratemykh Protsessovk Issledovaniiu Teplo-i Massoperenosa," Inzh. Fiz. Zh, Vol. 9, 1965, pp. 287-304.

13. Kaliski, S., "Wave Equation of Heat Conduction," Bulletin Academie Polonaise, Sci. Ser. Sci. Tech., Vol. 13, 1965, pp. 253-260.

14. Popov, E.B., "Dynamic Coupled Problem of Thermoelasticity for a Half-Space Taking Account of the Finiteness of the Heat Propagation Velocity," Journal of Applied Mathematics and Mechanics, Vol. 31, No. 2, 1967, pp. 349-356.

15. Lord, H.W. and Y. Shulman, "A Generalized Dynamical Theory of Thermoelasticity," Journal of Mechanics and Physics of Solids, Vol. 15, 1967, pp. 299-309.

16. Gurtin, M.E. and A.C. Pipkin, "A General Theory of Heat Conduction with Finite Wave Speeds," Archive for Rational Mechanics and Analysis, Vol. 31, 1968, pp. 113-126.

17. Nunziato, J.W., "On Heat Conduction in Materials with Memory," Quarterly of Applied Mathematics, Vol. 29, 1971, pp. 187-204.

18. Stolz Jr., G., "Numerical Solutions to an Inverse Problem of Heat Conduction for Simple Shapes," Journal of Heat Transfer, Trans. ASME, Series C, Vol. 82, 1960, pp. 20-26.

19. Liebert, C.H., J.E. Hatch and R.W. Grant, "Application of Various Techniques for Determining Local Heat Transfer Coefficients in a Rocket Engine from Transient Experimental Data," NASA Technical Note D-277, 1960.

20. Nestor, O.H. and H.N. Olsen, "Numerical Methods for Reducing Line and Surface Probe Data," SIAM Review, Vol. 2, No. 3, 1960, pp. 200-207.

21. Anderson, J.E. and E.F. Stresino, "Heat Transfer from Flames Impinging on Flat and Cylindrical Surfaces," Journal of Heat Transfer, Trans. ASME, Series C, Vol. 85, 1963, pp. 49-54.

22. Irving, F., "An Application of Least Squares Method to the Solution of the Inverse Problem of Heat Conduction," Journal of Heat Transfer, Trans. ASME, Series C, Vol. 85, 1963, pp. 378-379.

23. Powell, W.B. and T.W. Price, "A Method for the Determination of Local Heat Flux from Transient Temperature Measurements," ISA Transactions, Vol. 3, No. 3, 1964, pp. 246-254.

24. Burggraf, O.R., "An Exact Solution of the Inverse Problem in Heat Conduction Theory and Applications," Journal of Heat Transfer, Trans. ASME, Series C, Vol. 86, 1964, pp. 373-382.

25. Sparrow, E.M., A. Haji-Sheikh and T.S. Lundgren, "The Inverse Problem in Transient Heat Conduction," Journal of Applied Mechanics, Trans. ASME, Series E, Vol. 86, 1964, pp. 369-375.

26. Beck, J.V., "The Inverse Problem in Transient Heat Conduction," Journal of Applied Mechanics, Trans. ASME, Series E, Vol. 87, 1965, pp. 472-473.

27. Davies, J.M., "Input Power Determination from Temperatures in Simulated Skin Protected Against Thermal Radiation," Journal of Heat Transfer, Trans. ASME, Series C, Vol. 88, 1966, pp. 154-160.

28. Deverall, L.I. and R.S. Channopragada, "A New Integral Equation for Heat Flux in Inverse Heat Conduction," Journal of Heat Transfer, Trans. ASME, Series C, Vol. 88, 1966, pp. 327-328.

29. Kover'yanov, V.A., "Inverse Problem of Nonsteady-State Thermal Conductivity," Teplofizika Vysokiph Temperatur, Vol. 5, 1967, pp. 141-143.

30. Beck, J.V., "Surface Heat Flux Determination Using an Integral Method," Nuclear Engineering and Design, Vol. 7, 1968, pp. 170-178.

31. Beck, J.V., "Nonlinear Estimation Applied to the Nonlinear Inverse Heat Conduction Problem," International Journal of Heat and Mass Transfer, Vol. 13, 1970, pp. 703-716.

32. Anderson, S.A., L.A. Hale and P.E. Pulley, "A Technique for Determining the Transient Heat Flux at a Solid Interface Using the Measured Transient Interfacial Temperature," ASME Paper, No. 72-HT-18, 1972.

33. Schulte, E.H., "Impingement Heat-Transfer Rates from Torch Flames," Journal of Heat Transfer, Trans. ASME, Series C, Vol. 94, 1972, pp. 231-233.

34. Imber, M. and J. Khan, "Prediction of Transient Temperature Distributions with Embedded Thermocouples," AIAA Journal, Vol. 10, No. 6, 1972, pp. 784-789.

35. Imber, M., "A Temperature Extrapolation Method for Hollow Cylinders," AIAA Journal, Vol. 6, No. 1, 1973, pp. 117-118.

36. Tetelman, A.S. and A.J. McEvily Jr., Fracture of Structural Materials, John Wiley and Sons, Inc., New York, N.Y., 1967.

37. Jaeger, J.C., "Fracture of Rocks," The Proceedings of the First Tewksbury Symposium, held by the Faculty of the University of Melbourne, August 26-30, 1963.

38. McClintock, F.A. and J.B. Walsh, "Friction on Griffith Cracks in Rocks under Pressure," Proceedings Fourth U.S. Congress of Applied Mechanics, Berkeley, 1962, ASME, New York, 1963, pp. 1015-1021.

39. Bieniawski, Z.T., "Fracture Dynamics of Rock," International Journal of Rock Mechanics and Mining Science, Vol. 4, No. 4, 1968, pp. 415-429.

40. Chen, T.S. and R.L. Marovelli, "Analysis of Stresses in a Rock Disk Subjected to Peripheral Thermal Shock," Bureau of Mines Report of Investigations 6823, 1966.

41. Lindroth, D.P. and W.G. Krwazs, "Heat Content and Specific Heat of Six Rock Types at Elevated Temperatures up to 1000°C," Bureau of Mines Report of Investigations 7503, 1971.

42. Marovelli, R.L. and KF. Veith, "Thermal Conductivity of Rock: Measurement by the Transient Line Source Method," Bureau of Mines Report of Investigations 6604, 1965.

43. Thirumalai, K., "Potential of Internal Method for Rock Fragmentation," Proceedings of the 12th Symposium on Rock Mechanics, Held at the University of Missouri-Rolla, Rolla Missouri, November 16-18, 1970.

44. Lauriello, P.J.J., "Thermal Fracturing of Hard Crystalline Rock," Ph.D. Thesis, Rutgers University, 1971.

45. Kreith, F., Principles of Heat Transfer, International Textbook Company, Scranton, Pa., 1958.

46. Clark, G.B., et. al., "An Investigation of Thermal-Mechanical Fragmentation of Rock," University of Missouri-Rolla, RMERC, Annual Report, 1972.

47. Beck, J.V. and H. Hurwicz, "Effect of Thermocouple Cavity on Heat Sink Temperature," Journal of Heat Transfer, Trans. ASME, Series C, Vol. 82, 1960, pp. 27-36.

48. Beck, J.V., "Thermocouple Temperature Disturbance in Low Conductivity Materials," Journal of Heat Transfer, Trans. ASME, Series C, Vol. 84, 1962, pp. 124-132.

49. Beck, J.V., "Transient Sensitivity Coefficients for the Thermal Contact Conductance," International Journal of Heat Mass Transfer, Vol. 10, 1967, pp. 1615-1617.

50. Wilson, E.L. and R.E. Nickell, "Application of the Finite Element Method to Heat Conduction Analysis," Nuclear Engineering and Design, Vol. 4, No. 3., 1966, pp. 276-286.

51. Arpaci, V.S., Conduction Heat Transfer, Addison-Wesley Publishing Company, Reading, Mass., 1966.

52. Boyle, E.F. and A. Jennings, "Accelerating the Convergence of Elastic-Plastic Stress Analysis," International Journal for Numerical Methods in Engineering, Vol. 7, No. 2, pp. 232-235.

53. Keith, H.D., Personal Communication, University of Missouri-Rolla, Rolla, Missouri.

54. Gelfand, I.M., S.V. Fomin and R.A. Silverman (translator), Calculus of Variations, Prentice-Hall, Inc., Englewood Cliffs, N.J., 1963.

55. Sidles P.H. and G.C. Damielson, "Thermal Diffusivity Metals at High Temperature," Journal of Applied Physics, Vol. 25, No. 1, 1954, pp. 58-66.

56. Touloukian, Y.S., et. al., Thermophysical Properties of Matter: The TPRC Series, Vol. 1. Thermal Conductivity: Metallic Elements and Alloys, IFI/Plenum, New York, 1970, pp. 697-699.

57. Touloukian, Y.S., et. al., Thermophysical Properties of Matter: The TPRC Series, Vol. 4, Specific Heat: Metallic Elements and Alloys, IFI/Plenum, New York, 1970, pp. 392-397.

58. Scheller, J.D., "Thermal Fragmentation of Rocks-Influence of Temperature Dependent Material Properties," M.S. Thesis, University of Missouri-Rolla, 1974.

VITA

Vernon Dale Allen was born on January 5, 1941, in Piedmont, Missouri. He received his primary and secondary education in St. Louis, Missouri. He has received his college education from Harris Teachers College in St. Louis, Missouri and Washington University in St. Louis, Missouri. He received a Bachelor of Science degree in Mechanical Engineering from Washington University in St. Louis, Missouri, in June 1962.

He worked for the United States Army in St. Louis, Missouri from June 1962 until he entered the United States Air Force in March 1963. After completing military service in June 1967, he returned to work for the United States Army AVSCOM. In January 1969 he enrolled in the graduate school of the University of Missouri-Rolla, where he received his Master of Science degree in May 1971.

In December 1973 he married Miss Cheryl Lee Breig in St. Louis, Missouri.

APPENDIX A

THERMAL ANALYSIS PROGRAM

2DNLT - INPUT INSTRUCTIONS

This program was developed for thermal analysis of plane or axisymmetric bodies with temperature dependent material properties and time dependent heat flux or temperature boundary conditions. Thermal properties are assumed functions of temperature in the form:

$$\text{Conductivity} = K_0 + K_1T + K_2T^2 + K_3T^3$$

$$\text{Heat Capacity} = C_0 + C_1T + C_2T^2 + C_3T^3$$

Density = Constant

Other equations for conductivity and heat capacity can be substituted into 2DNLT by a simple modification. Scheller (58) substituted different equations into 2DNLT for his research.

Normally any consistent set of units can be used with a finite element program. One copy of 2DNLT was labeled (2DNLT - Special) and this program used thermal resistivity as a cubic function of temperature instead of thermal conductivity. 2DNLT - Special converted the resistivity to conductivity and changed the units from British units to metric units.

A. Transient Analysis

The following set of cards is required for each problem to be analyzed.

1. Identification Card (36A2):

Columns	1-72	This card is used to identify the problem being analyzed.

2. Control Card (7I5,E15.6, F5.0, 2I5, F10.0):

Columns	1-5	Number of nodal points (100 maximum)
	6-10	Number of elements (100 maximum)
	11-15	Number of convection boundary conditions (100 maximum)
	16-20	Geometry option, 0 for plane problem 1 for axisymmetric problem
	21-25	Number of different materials (4 maximum)
	26-30	Number of time increments
	31-35	Print out interval
	36-50	Time interval size
	51-55	Print input data option, 0.0 no print 1.0 print input data
	56-60	Material property iteration option, program defaults to four iterations
	61-65	Number of boundary nodal points that are time dependent

66-75 Reference temperature, initial temperature of body

3. Material Property Cards The following group must be supplied for each material.

a) First Card (I10, 4F10.0):

Columns 1-10 Material identification number

11-20 Reference temperature conductivity

21-30 Reference temperature heat capacity

31-40 Density

41-50 Rate of heat generation per unit volume

b) Second Card (4F20.5) Coefficients of conductivity equation

Columns 1-20 Constant coefficient

21-30 Linear coefficient

31-40 Quadratic coefficient

41-50 Cubic coefficient

c) Third Card (4F20.5) Coefficients of heat capacity equation

Columns 1-20 Constant coefficient

21-30 Linear coefficient

31-40 Quadratic coefficient

41-50 Cubic coefficient

. Nodal Point Cards (2I5, 3F10.0):

Columns	1-5	Nodal point number
	10	Specified temperature or flux option, 0 specified heat flow 1 specified temperature
	11-20	X or R coordinate
	21-30	Y or Z coordinate
	31-40	Specified heat flow or temperature (For an axisymmetric body the total heat flow on a one radian segment)

Nodal point cards are input in numerical sequence. Omitted nodal point cards are generated at equal intervals along a straight line between the specified nodal points. For generated nodes the heat flow is specified as zero.

The coordinate system (X,Y or R,Z) must be a right handed system.

5. Element Cards (6I5):

Columns	1-5	Element number
	6-10	Nodal point I
	11-15	Nodal point J
	16-20	Nodal point K
	21-25	Nodal point L (Blank or L=K indicates a triangular element)

26-30 Material identification number (Default to material number 1)

Nodal point numbers (I,J,K,L) must be ordered in a counter clockwise direction around each element. Maximum difference between nodal points is 10.

Element cards are input in numerical sequence. Omitted element cards are generated by incrementing the nodal numbers of the previous element. The material identification number for generated elements is the same as the previous element material identification number.

6. Convection Boundary Cards (2I5, 2F10.0) One card must be supplied for each boundary element.

Columns 1-5 I boundary nodal point
6-10 J boundary nodal point
11-20 Convective coefficient h
21-30 Temperature of external fluid

7. Time Dependent Boundary Cards (F10.0) One card with the surface condition for the beginning of each time interval and the one card with the ending value for the last time interval. The time dependent boundary (either temperature or flux) is fixed for each time interval but is allowed to change between intervals. The beginning surface value card for the time interval

being analyzed is averaged with the beginning surface value for the next time interval to obtain the current boundary value.

B. Steady State Analysis

The 2DNLT program could be used for steady state analysis, however, the storage requirements for a steady state analysis are much smaller such that the program is inefficient for a steady state analysis. An additional program available at the RMERC called 2DNSS1, contains the steady state version of the 2DNLT program. The input is the same except for the following:

1. Control Card:

   Columns 26-50 Blank

2. Material Property Cards:

   a) First Card:

      Columns 21-40 Blank

   b) Third Card: (omit)

3. Time Dependent Boundary Cards: (omit)

APPENDIX B

SURFACE IMPROVEMENTS

Equation (3.24) was evaluated for four possible boundary condition improvement assumptions.

A. Linear dg Assumption

A linear assumption of dg can be expressed as

$$dg = dg_0 + m(t-a) \qquad a \leq t \leq b \tag{A-1}$$

where

$$dg_0 \neq dg_0(t) = \text{constant} \tag{A-2}$$

$$m \neq m(t) = \text{constant} \tag{A-3}$$

Substituting dg in Equation (3.24)

$$\int_a^b \left(\frac{\partial T^{\ell}}{\partial g}\right)^2 \left(dg_0 + m(t-a) \right) dt = \int_a^b (Y-T^{\ell}) \frac{\partial T^{\ell}}{\partial g} dt \tag{A-4}$$

or

$$dg_0 \int_a^b \left(\frac{\partial T^{\ell}}{\partial g}\right)^2 dt + m \int_a^b \left(\frac{\partial T^{\ell}}{\partial g}\right)^2 (t-a)\, dt = \int_a^b (Y-T^{\ell}) \frac{\partial T^{\ell}}{\partial g} dt \tag{A-5}$$

There are two unknowns in Equation (A-5) and the solution of the inverse with two unknowns is not possible. If

either dg or m is known, then the other one can be found.

1. Slope m of dg Known If the slope of dg is known, then Equation (A-5) becomes

$$dg_0 = \frac{\int_a^b (Y-T^\ell)\ \frac{\partial T^\ell}{\partial g}\ dt - m \int_a^b (\frac{\partial T^\ell}{\partial g})^2 (t-a)\ dt}{\int_a^b (\frac{\partial T^\ell}{\partial g})^2\ dt} \qquad \text{(A-6)}$$

2. Starting Value of dg Known If dg is known, then Equation (A-5) becomes

$$m = \frac{\int_a^b (Y-T^\ell)\ \frac{\partial T^\ell}{\partial g}\ dt - dg \int_a^b (\frac{\partial T^\ell}{\partial g})^2\ dt}{\int_a^b (\frac{\partial T^\ell}{\partial g})^2\ (t-a)\ dt} \qquad \text{(A-7)}$$

B. Step Changes in dg

This boundary condition improvement is a constant for one time period and another constant for a second time period.

$$dg = dg_0 \qquad a \leq t \leq t_1 \qquad \text{(A-8)}$$

$$dg = dg_1 \qquad t_1 \leq t \leq b \qquad \text{(A-9)}$$

Substituting into Equation (3.24)

$$\int_a^{t_1} (\frac{\partial T^\ell}{\partial g})^2 dg_0\ dt + \int_{t_1}^b (\frac{\partial T^\ell}{\partial g})^2\ dg_1\ dt$$

$$= \int_a^b (Y-T^\ell)\ \frac{\partial T^\ell}{\partial g}\ dt \qquad \text{(A-10)}$$

If either dg_0 or dg_1 is known then the other can be found.

1. $\underline{dg_0}$ $\underline{\text{Known}}$ If dg_0 is known, then dg_1 can be expressed as

$$dg_1 = \frac{\int_a^b (Y-T^{\ell}) \left(\frac{\partial T^{\ell}}{\partial g}\right) dt - dg_0 \int_a^{t_1} \left(\frac{\partial T^{\ell}}{\partial g}\right)^2 dt}{\int_{t_1}^b \left(\frac{\partial T^{\ell}}{\partial g}\right)^2 dt} \qquad \text{(A-11)}$$

2. $\underline{dg_1}$ $\underline{\text{Known}}$ If dg_1 is known the dg_0 can be expressed as

$$dg_0 = \frac{\int_a^b (Y-T^{\ell}) \left(\frac{\partial T^{\ell}}{\partial g}\right) dt - dg_1 \int_{t_1}^b \left(\frac{\partial T^{\ell}}{\partial g}\right)^2 dt}{\int_a^{t_1} \left(\frac{\partial T^{\ell}}{\partial g}\right)^2 dt} \qquad \text{(A-12)}$$

APPENDIX C

INVERSE THERMAL ANALYSIS PROGRAM

INVRS - INPUT INSTRUCTIONS

This program was developed for the inverse thermal analysis of plane or axisymmetric bodies with temperature dependent material properties. Iteration is performed with the 2DNLT program. The input for INVRS is very similar to the input for 2DNLT. Thermal properties are assumed functions of temperature in the form:

Conductivity = $K_0 + K_1T + K_2T^2 + K_3T^3$

Heat Capacity = $C_0 + C_1T + C_2T^2 + C_3T^3$

Density = Constant

Normally any consistent set of units can be used with a finite element program.

One copy of the INVRS program was labeled (INVRS - Special) and this program used thermal resistivity as a cubic function of temperature instead of thermal conductivity. INVRS - Special converted the resistivity to conductivity and changed the units from British units to metric units.

The inverse solution is found by iteration and the material properties are updated after each iteration. The iteration is completed when the solution for each time step changes less than .5% between iterations.

When using future times, iteration between time steps

may be required. The number of material property iterations must be specified.

A. Transient Analysis

The following set of cards is required for each problem to be analyzed.

1. Identification Card (36A2):

Columns	1-72	This card is used to identify the problem being analyzed.

2. Control Card (7I5, E15.6, F5.0, I5, F10.0):

Columns	1-5	Number of nodal points (500 maximum)
	6-10	Number of elements (500 maximum)
	11-15	Number of convective boundary conditions (500 maximum)
	16-20	Geometry option, 0 for plane problem 1 for axisymmetric problem
	21-25	Number of different materials (4 maximum)
	26-30	Number of time increments
	31-35	Print out interval
	36-50	Time interval size
	51-55	Print input data option, 0.0 no print 1.0 print input data

56-60 Material property iteration option, program defaults to no iterations

61-70 Reference temperature, initial temperature of body

3. Material Property Cards The following group must be supplied for each material.

a) First Card (I10, 4F10.0):

Columns 1-10 Material identification number

11-20 Reference temperature conductivity

21-30 Reference temperature heat capacity

31-40 Density

41-50 Rate of heat generation per unit volume

b) Second Card (4F20.5) Coefficients of conductivity equation

Columns 1-20 Constant coefficient

21-30 Linear coefficient

31-40 Quadratic coefficient

41-50 Cubic coefficient

c) Third Card (4F20.5) Coefficients of heat capacity equation

Columns 1-20 Constant coefficient

	21-30	Linear coefficient
	31-40	Quadratic coefficient
	41-50	Cubic coefficient

4. Nodal Point Cards (2I5, 3F10.0):

Columns	1-5	Nodal point number
	10	Specified temperature or flux option, 0 specified heat flow 1 specified temperature
	11-20	X or R coordinate
	21-30	Y or Z coordinate
	31-40	Specified heat flow or temperature (For an axisymmetric body the total heat flow on a one radian segment)

Nodal point cards are input in numerical sequence. Omitted nodal point cards are generated at equal intervals along a straight line between the specified nodal points. For generated nodes the heat flow is specified as zero.

The coordinate system (X,Y or R,Z) must be a right handed system.

5. Element Cards (6I5):

Columns	1-5	Element number
	6-10	Nodal point I
	11-15	Nodal point J

16-20 Nodal point K

21-25 Nodal point L (Blank or L=K indicates a triangular element)

26-30 Material identification number (Default to material number 1)

Nodal point numbers (I,J,K,L) must be ordered in a counter clock direction around each element. Maximum difference between nodal point numbers is 20.

Element cards are input in numerical sequence. Omitted element cards are generated by incrementing the nodal numbers of the previous element. The material identification number for generated elements is the same as the previous element material identification number.

6. Convection Boundary Cards (2I5, 2F10.0) One card must be supplied for each boundary element.

Columns 1-5 I boundary nodal point

6-10 J boundary nodal point

11-20 Convective coefficient h

21-30 Temperature of external fluid

7. Control Card for Inverse Solution (5I5, F10.0):

Columns 1-5 Number of future times (Defaults to no future times)

6-10 Number of measured points (Defaults to one measured

point. Maximum number is 4.)

11-15	Maximum number of iterations per time step (Defaults to 20 iterations)
16-20	Number of material property iterations with a time step (Defaults to no iterations)
21-25	Number of nodal points on the boundary with the unknown surface function (Defaults to two nodal points)
26-35	Parameter to check convergence of solution (Default .5%)

8. Unknown Surface Function Nodal Points (10I5) Input the points along the boundary that the unknown surface function is on. Input ten nodal point numbers per card.

9. Measured Data Nodal Points (10I5) Input ten nodal points per card.

10. Measured Internal Temperatures (MF10.0) One card for each time interval in the solution. The input format will accept up to four measured points per card.

Columns	1-5	First measured nodal point temperature
	6-10	Second measured nodal point

	temperature
11-15	Third measured nodal point
	temperature (If required)
16-20	Fourth measured nodal point
	temperature (If required)

APPENDIX D

EXPERIMENTAL EQUIPMENT AND WIRING DIAGRAMS

This appendix consists of lists of equipment, a general layout sketch, a general electrical block diagram and wiring diagrams for the circuits designed and built in the RMERC.

LIST OF EQUIPMENT

DC Micro Volt ammeter	model 425 AR, Hewlett Packard, Palo Alto, Calif.
Watt meter	model Univ. NOU 21673, Sensitive Research, The Singer Co., Bridgeport, Conn.
Eight channel recorder	Speedomax G, Leeds & Northrup Co., Philadelphia, Penn.
Two channel recorder	Speed Servo II, Easterline Angus
Strain gage	WK-03-500BH-350 with option B87, Micro-Measurements, Romulus, Mich.

Temperature Gage	BLH type RTP-50-F10 resistance gage, BLH Electronics, Waltham, Mass.
Thermocouple wire	SPCH-005 chromel wire, SPAL-005 alumel wire, Omega Engineering, Stanford, Conn.
Power control	Transtat voltage regulator, Radio Engineering Laboratories, American Transformer Division, New York, N.Y.
Power switch	115 Volts, 30 amps., General Electric, purchased locally

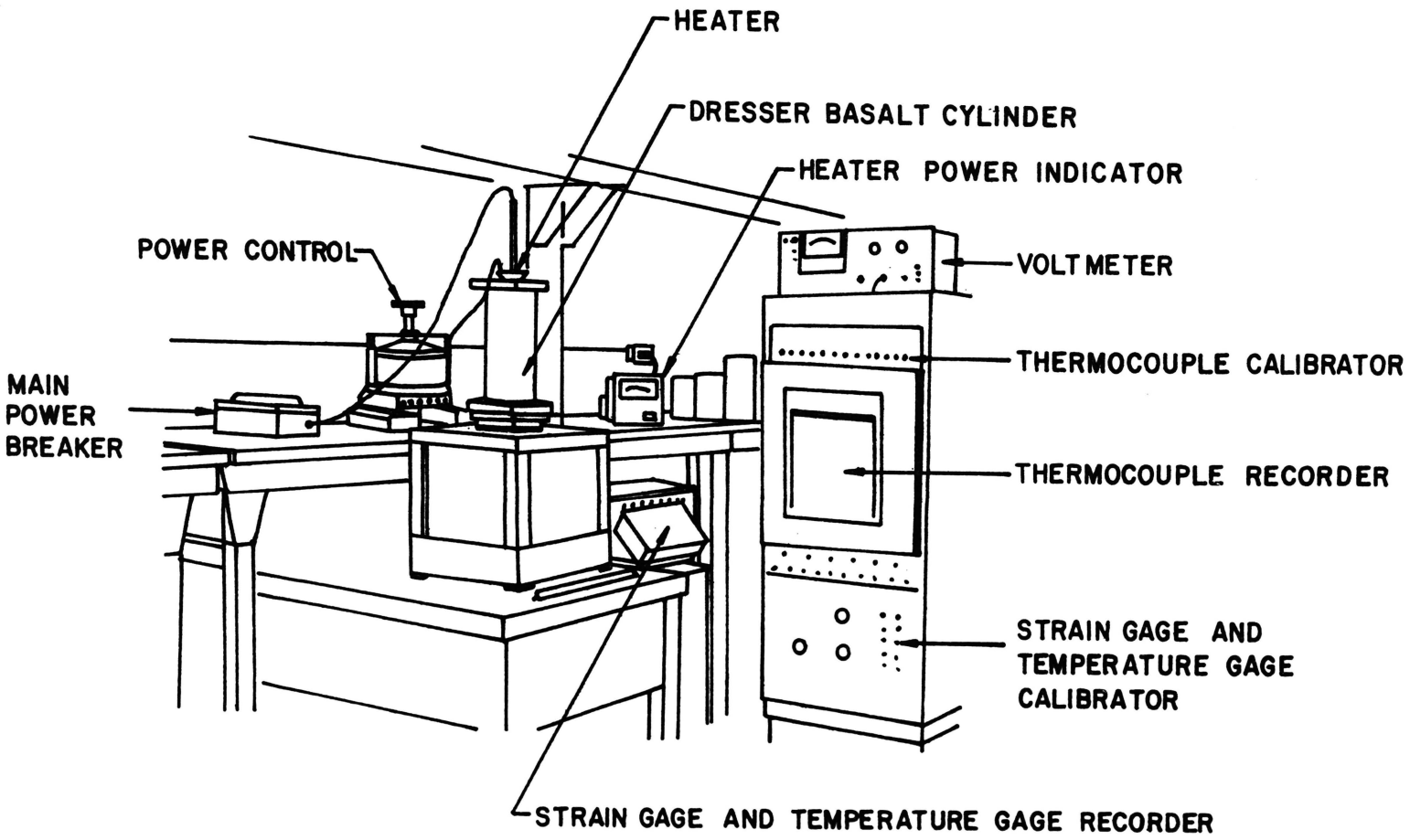

Figure 24 General Equipment Layout

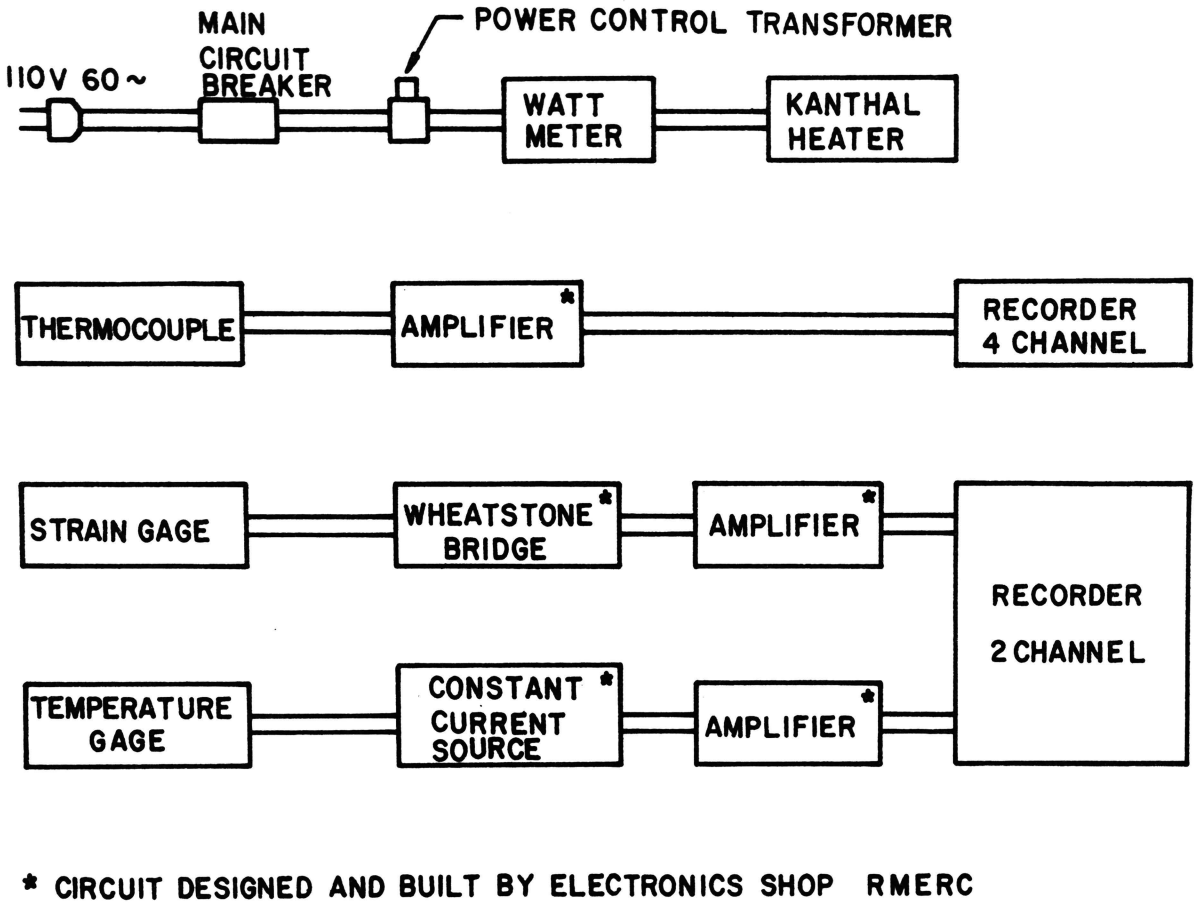

Figure 25 General Electrical Block Diagram

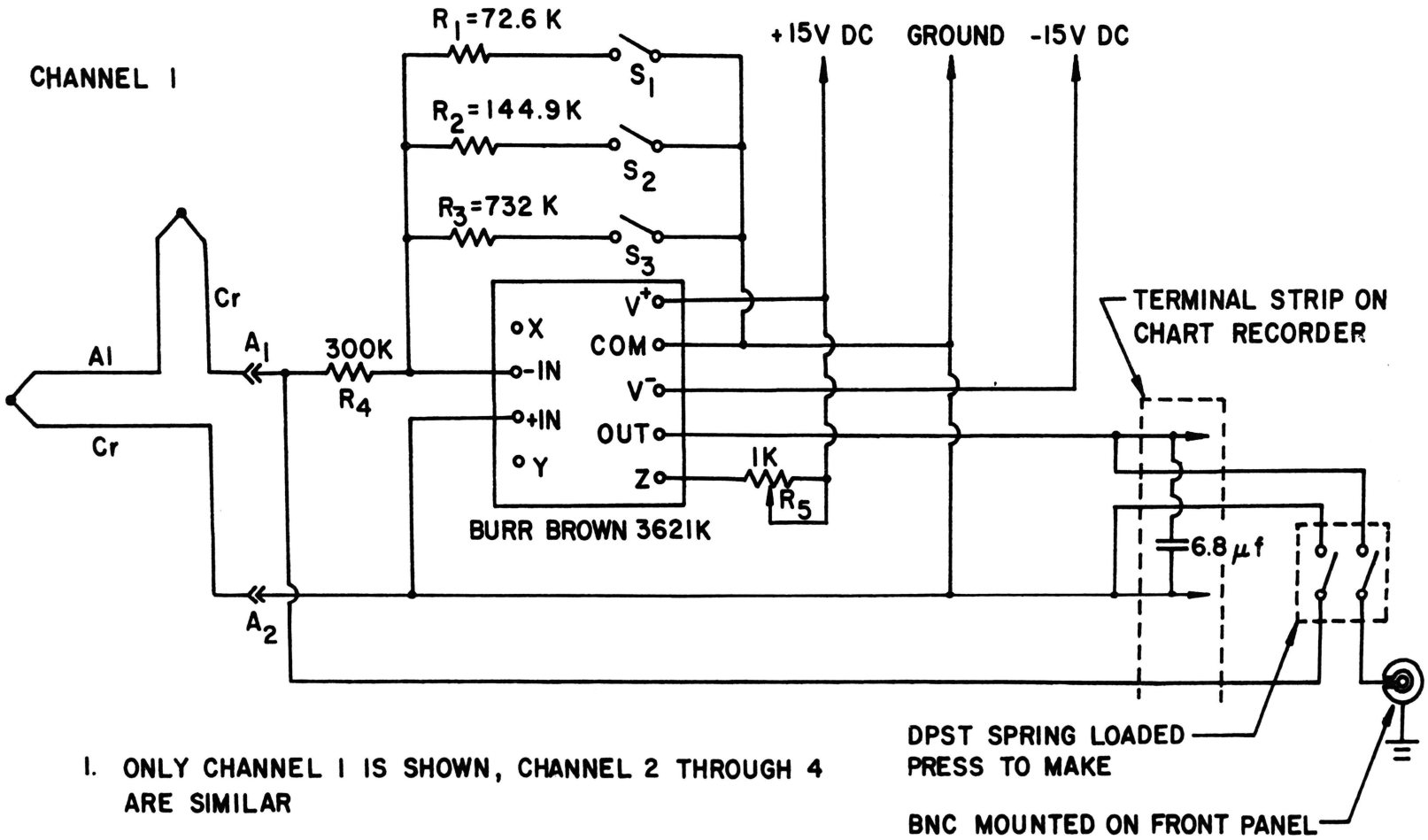

1. ONLY CHANNEL 1 IS SHOWN, CHANNEL 2 THROUGH 4 ARE SIMILAR
2. A_1 & A_2 ARE THERMOCOUPLE CONNECTIONS
3. ONE THERMOCOUPLE IS PLACED INSIDE THE TEST SPECIMEN AND ONE THERMOCOUPLE IN AN ICE-WATER MIXTURE

Figure 26 Thermocouple Schematic

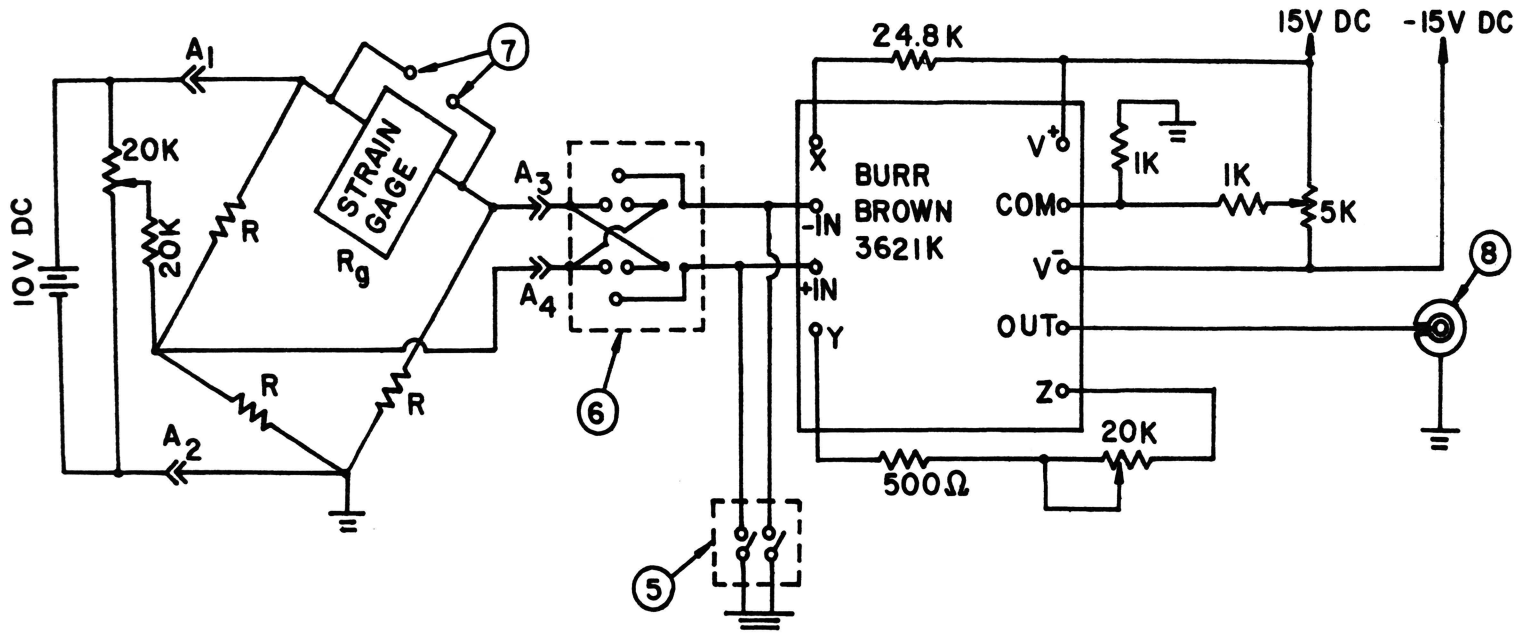

① A_1 THROUGH A_4 ARE STRAIN GAGE CONNECTORS

② THE COMPLETION RESISTORS FOR THE BRIDGE ARE TO BE MOUNTED ON A TERMINAL STRIP AS CLOSE TO THE STRAIN GAGE AS POSSIBLE

③ USE SHIELDED CABLE (STRAIN GAGE CABLE) TO GO FROM UNIT TO TERMINAL STRIP

④ R_1 THROUGH R_4 ARE LABELED ON CIRCUIT BOARD

⑤ DPST (SPRING LOADED) PRESS TO MAKE MOUNTED ON FRONT PANEL

⑥ DPDT, TENSION COMPRESSION SWITCH, MOUNTED ON FRONT PANEL

⑦ BANANA MOUNTED ON FRONT PANEL

⑧ BNC MOUNTED ON FRONT PANEL

Figure 27 Strain Gage Schematic

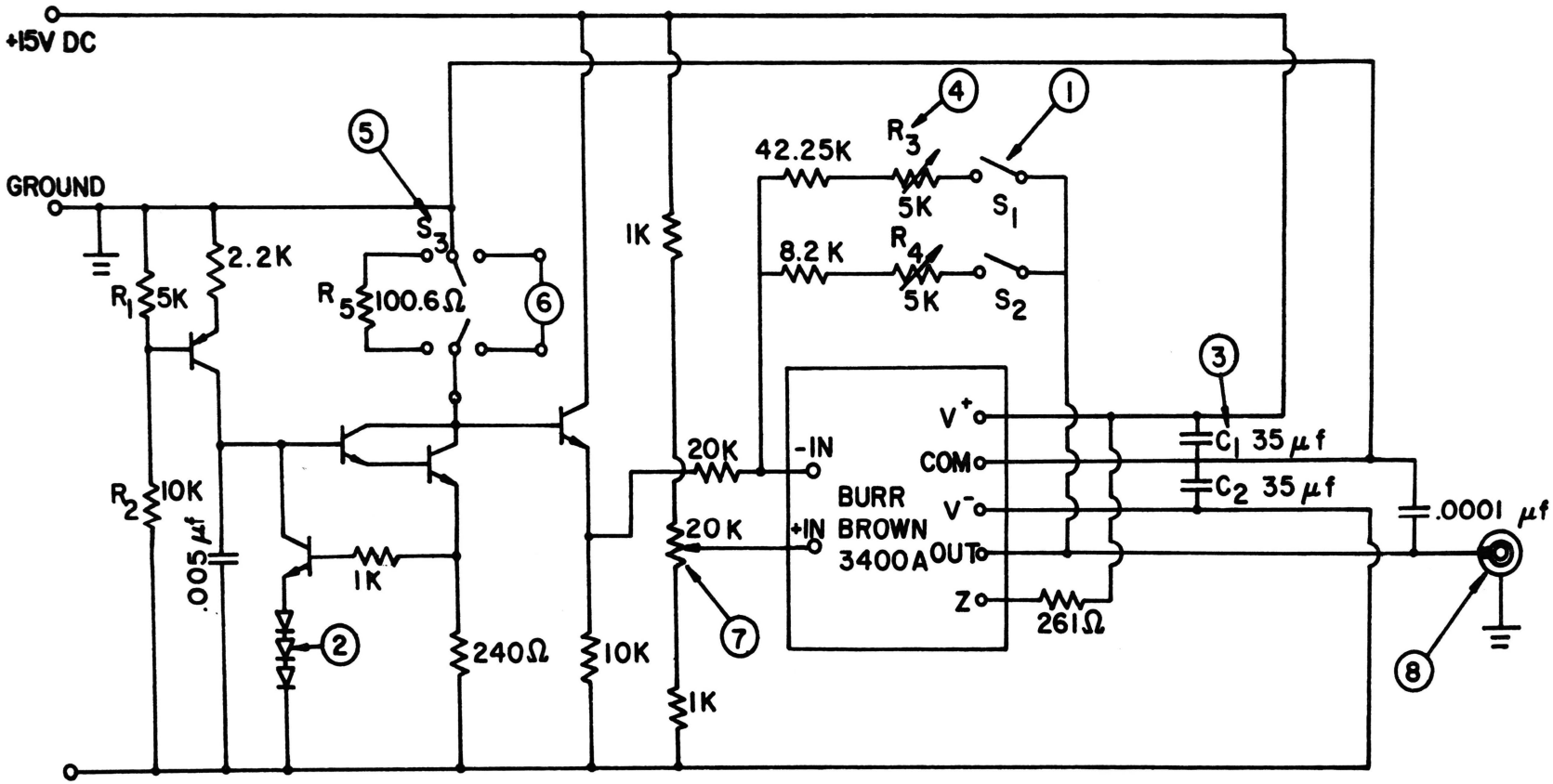

(1) S_1 & S_2 MOUNTED ON FRONT PANEL

(2) USE Si DIODES , Veb=.6 Volts

(3) C_1 & C_2 ARE PLACED CLOSE TO THE AMPLIFIER

(4) R_3 & R_4 ARE LABELED ON THE CIRCUIT BOARD

(5) DPDT SPRING LOADED PRESS TO CONNECT R_5 INTO CIRCUIT

(6) BANANA MOUNT ON FRONT PANEL, TEMPERATURE GAGE INPUT

(7) ZERO ADJUST MOUNTED ON FRONT PANEL

(8) BNC MOUNTED ON FRONT PANEL

Figure 28 Temperature Gage Schematic